

Electrospinning and Functionalization of Cellulose Acetate Nanofibre

by

Sushmita Majumder

Roll Number: 0417112011

MASTER OF SCIENCE IN MATERIALS AND METALLURGICAL
ENGINEERING

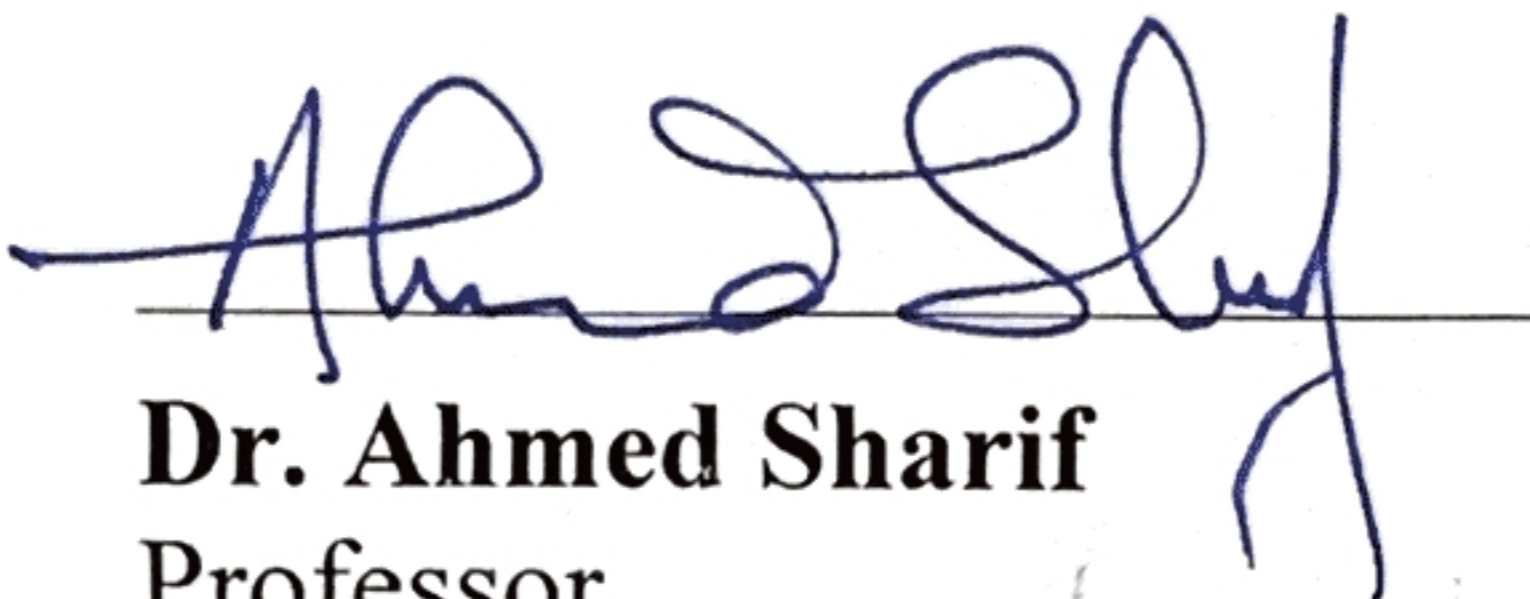
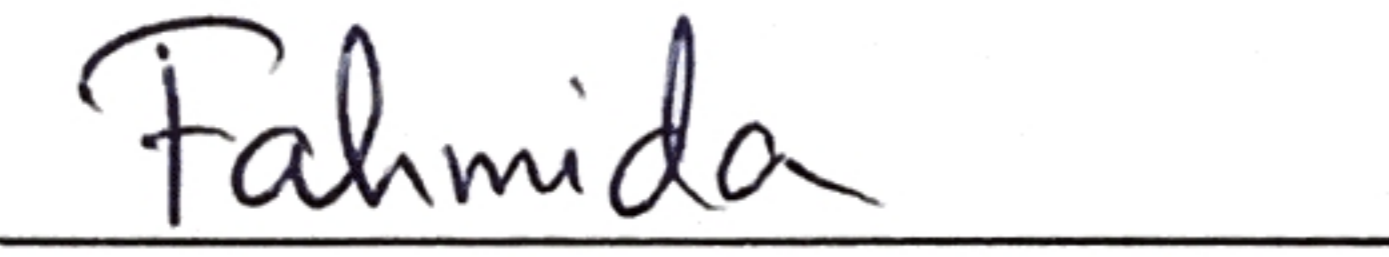

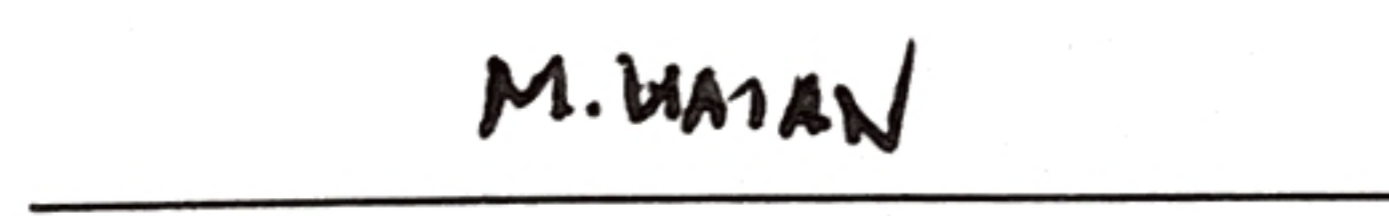
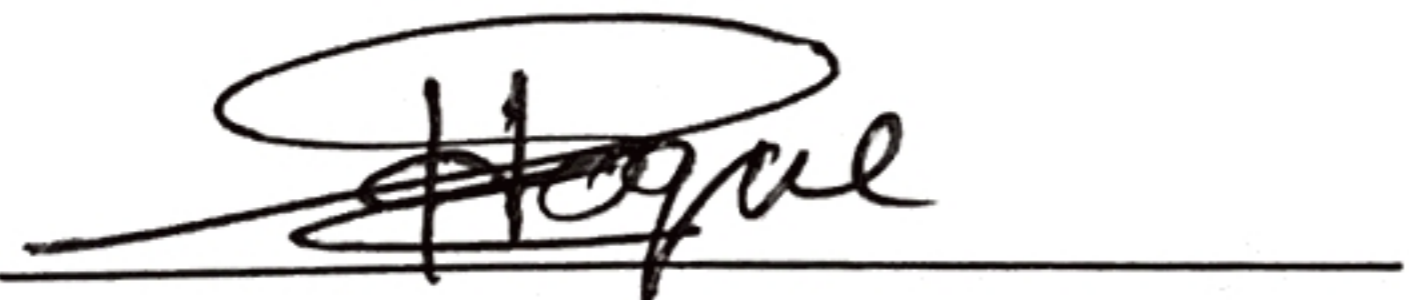


Department of Materials and Metallurgical Engineering
BANGLADESH UNIVERSITY OF ENGINEERING AND TECHNOLOGY (BUET)

June, 2019

The thesis titled “**Electrospinning and Functionalization of Cellulose Acetate Nanofibre**” Submitted by Sushmita Majumder, Roll No. 0417112011 and Session: April 2017 has been accepted as satisfactory as a partial fulfilment of the requirement for the degree of M.Sc.Engg. in Materials and Metallurgical Engineering on June 29, 2019

BOARD OF EXAMINERS

1. 
Dr. Ahmed Sharif
Professor
Department of Materials and Metallurgical Engineering, BUET
Chairman
(Supervisor)
2. 
Dr. Fahmida Gulshan
Professor and Head
Department of Materials and Metallurgical Engineering, BUET
Member
(Ex-officio)
3. 
Dr. Kazi Md. Shorowordi
Professor
Department of Materials and Metallurgical Engineering, BUET
Member
4. 
Dr. Mahbub Hasan
Professor
Department of Materials and Metallurgical Engineering, BUET
Member
5. 
Dr. Md. Enamul Hoque
Professor
Department of Biomedical Engineering
Mirpur Cantonment, MIST, Dhaka 1216
Member
(External)

DECLARATION

Declared that except where specified by reference to other works, the experimental studies embodied in this thesis is the result of investigation carried out by the author. Neither the thesis nor any part has been submitted to or is being submitted elsewhere for any other purposes.

Signature of the student


Sushmita Majumder

TABLE OF CONTENTS

List of Tables	vii
List of Figures	viii
Acknowledgement	x
Abstract	xi
Chapter 1: Introduction	1
1.1 Background and Research Significance.....	1
1.2 Objectives of the Present Study.....	1
1.3 Organization of the Thesis.....	2
Chapter 2: Literature Review	3
2.1 Electrospinning.....	3
2.1.1 History of electrospinning.....	3
2.1.2 Electrospinning fundamentals.....	4
2.1.3 Electrospinning parameter investigation.....	6
2.1.4 Applications of electrospinning.....	8
2.2 Polymers Used In Electrospinning.....	12
2.3 Cellulose Acetate (CA): A Potential Polymer in Electrospinning...	13
2.4 Polyethylene Glycol (PEG).....	16
2.4.1 Polyethylene glycol as a modifier.....	16
2.4.2 Polyethylene glycol as a stabilizer.....	17
2.5 Wound Dressings.....	18
2.5.1 Traditional wound dressing.....	18
2.5.2 Modern wound dressing.....	18
2.5.3 Electrospun fibres as wound dressing.....	19
2.6 Silver: An Antibacterial Agent In Electrospun Fibre Mat.....	20
2.6.1 Synthesis routes of silver nanoparticles.....	22
2.6.2 Mechanisms of silver's antibacterial properties.....	25

Chapter 3: Experimental Overview.....	28
3.1 Materials.....	28
3.2 Preparation of CA Solutions.....	28
3.3 Preparation of CA Solutions with PEG and AgNO ₃	29
3.4 Electrospinning of CA Solutions into Fibre.....	30
Chapter 4: Electrospinning of Cellulose Acetate Using Different Solvent Systems.....	33
4.1 Introduction.....	33
4.2 Experimental.....	34
4.2.1 Materials.....	34
4.2.2 Electrospinning of CA nanofibers.....	34
4.2.3 Characterization of electrospun CA nanofibers.....	34
4.3 Results and Discussion.....	35
4.3.1 Solubility and spinnability.....	35
4.3.2 Viscoelastic properties of the CA solution.....	39
4.3.3 Morphological study of electrospun CA fibre.....	43
4.3.4 Effects of electrical conductivity of solution.....	44
4.3.5 ATR-FTIR.....	45
Chapter 5: Electrospinning and Modification of Cellulose Acetate Fibre with Polyethylene Glycol.....	47
5.1 Introduction.....	47
5.2 Materials and Methods.....	47
5.2.1 Materials.....	47
5.2.2 Preparation of solutions and electrospinning of nanofibrous mat.....	47
5.2.3 Nanofibres characterization.....	48
5.2.4 Swelling measurements.....	48
5.3 Results And Discussion.....	48
5.3.1 Structural analysis.....	48

5.3.2 Morphological analysis.....	49
5.3.3 Thermal analysis.....	51
5.3.4 Swelling behaviour analysis.....	52
Chapter 6: Functionalization of CA fibre with AgNO₃ and Assessment of Antibacterial Activity.....	54
6.1 Introduction.....	54
6.2 Materials and Methods.....	55
6.2.1 Materials.....	55
6.2.2 Preparation of solutions and electrospinning of nanofibrous mat with AgNO ₃	55
6.2.3 CA-PEG-Ag nanofibres characterization.....	55
6.2.4 Antibacterial evaluation.....	56
6.3 Results And Discussion.....	57
6.3.1 Structural analysis.....	57
6.3.2 Morphological analysis.....	57
6.3.3 UV-Vis analysis.....	58
6.3.4 Mechanical property analysis.....	59
6.3.5 Thermal property analysis.....	61
6.3.6 Antibacterial assay.....	62
Chapter 7: Summary of the Results.....	64
Chapter 8: Conclusion and Recommendation.....	67
8.1 Findings of the Present Research Work.....	67
8.2 Scope for Future Investigation.....	68
Bibliography.....	69

LIST OF TABLES

Table No.	Table Content	Page No.
2.1	Different polymers used in electrospinning and their applications	13
2.2	Summary of Ag nanoparticles in antibacterial study	21
3.1	Variation of electrospinning and solution parameters to obtain fibre	30
4.1	Hansen solubility parameters for CA and solvents	36
7.1	Comparisons of electrical conductivity	64
7.2	Comparisons of morphological structures	64
7.3	Comparisons of mechanical property	66
7.4	Comparisons of swelling property	66
7.5	Comparisons of antibacterial property	66

LIST OF FIGURES

Fig. No.	Figure Title	Page No.
2.1	Schematic setup of electrospinning	5
2.2	Nanofibre mat for wound dressing	9
2.3	Drug delivery through polymer nanofiber	10
2.4	Artificial blood vessel	11
2.5	Chemical Structure of CA	14
2.6	Applications of CA fibres in different arena	15
2.7	Diagram summarizing nano-scaled silver interaction with bacterial cells	26
3.1	Clear, viscous 17 wt% CA solution in 3:1 acetic acid/water stirred for 4 hrs	28
3.2	17 wt% CA in (a) water and (b) 100% acetic acid	29
3.3	CA solution in 2:1 acetone/DMAc (a) before and (b) after adding AgNO ₃	29
3.4	Collected CA fibre mat after electrospinning	32
3.5	Schematic of electrospinning of CA fibre mat	32
4.1	Teas chart to analyze feasibility of solution formation and spinning with different solvents for CA	38
4.2	Viscoelasticity measurement of CA solutions	40
4.3	Relationship between shear stress and shear rate of CA solutions with varied concentrations and solvent systems	40
4.4	Different needle tip conditions showing (a) clogging of needle tip for CA in pure acetone (b) bending elongation of jet for 10 and 12 wt% CA in 3:1 acetic acid/water and (c) forming of stable cone for 15, 17 and 19 wt% CA in binary solvents	41
4.5	SEM images of (a) 10 (b) 12 and (c) 15 wt% CA in 3:1 acetic acid/water	42

4.6	SEM images and fibre size distributions of 17 wt% CA in (a) 3:1 acetic acid/water (b) 2:1 acetone/DMAc and (c) pure acetone ; 19 wt% CA in (d) 3:1 acetic acid/water (e) 2:1 acetone/DMAc and (f) pure acetone	43
4.7	Electrical conductivity measurement device	44
4.8	Electrical conductivity of CA for different concentrations and solvent systems	45
4.9	ATR-FTIR device	46
4.10	ATR-FTIR spectrum of (a) CA-acetic acid (b) CA-acetone/DMAc and (c) CA-pure acetone	46
5.1	ATR-FTIR spectra of (a) pure CA (b) CA-PEG 200 and (c) CA-PEG 6000	49
5.2	FESEM (10000X) of fibres electrospun in a) CA-solvent b) CA-solvent-10wt% PEG 200 c) CA-solvent-20wt% PEG 200 d) CA-solvent-40wt% PEG 200 e) CA-solvent-80wt% PEG 200 and f) CA-solvent-10wt% PEG 6000.	50
5.3	DSC thermogram of (a) CA-solvent (b) CA-10%PEG 200 (c) CA-20%PEG 200 (d) CA-40%PEG 200 fibre	52
5.4	Water uptake of different fibre mats at 1 and 24 hr	53
6.1	(a) Agar solution (b) Nutrient broth solution	56
6.2	ATR-FTIR spectra of (a) Pure CA, (b) CA-PEG 200 (c) CA-PEG 6000 and (d) CA-PEG 200-Ag	57
6.3	FESEM of CA-PEG-Ag fibre (a) 10000X (b) 100000X and (c) EDX of CA-PEG-Ag fibre	58
6.4	UV-Vis spectrophotometer	59
6.5	UV-Vis spectrum of CA-PEG 200 nanofibre containing 1 wt% AgNO ₃	59
6.6	Failure of the CA fibre mat during tensile test	60
6.7	(a) Stress vs strain plot for CA fibres (b) Tensile modulus diagram for CA, CA-PEG 200 and CA-PEG-Ag fibres	61

6.8	DSC thermogram of (a) CA, (b) CA-PEG 200 and (c) CA-PEG-Ag fibre	62
6.9	Antibacterial test results for (a) <i>E. coli</i> blank control (b) <i>E. coli</i> incubated with CA-PEG 200 fibre (c) <i>E. coli</i> blank control (d) <i>E. coli</i> incubated with Ag loaded CA-PEG 200 fibre (e) <i>S. aureus</i> blank control (f) <i>S. aureus</i> incubated with Ag loaded CA-PEG 200 fibre	63

ACKNOWLEDGEMENT

First, I would like to express my sincerest gratitude to the Almighty, the benevolent and the merciful, for His graciousness, unlimited kindness and divine blessings.

I would like to express my humble gratitude and sincere thanks to my thesis supervisor, Dr Ahmed Sharif, Professor, Department of Materials and Metallurgical Engineering, BUET for his adept guidance and enthusiastic support throughout the progress of this thesis.

I pay my utmost gratitude to Dr Muhammad Tarik Arafat, Assistant Professor, Department of Biomedical Engineering, BUET for his constant and priceless help with all the technical, theoretical and experimental aspects of this research project. I am truly indebted to him for giving me a direction in pursuing my interest to work on biomaterials. His constant and vigilant guidance and support for using his laboratory facilities has enabled me to bring novelty in this work.

I would like to thank Prof. Dr. Abdul Matin, Assistant Professor and Head, GCE for the allowance to use the characterization facilities.

A special thanks goes to Musavvir Mahmud Seazon, my friend and research assistant at Department of Biomedical Engineering of BUET, for helping me unconditionally with the involving procedures of antibacterial tests and lending a helping hand whenever needed.

I convey my regards to Mr. Rana of GCE for his technical support throughout the endeavour, and to the staffs and members of MME for providing us assistance whenever it was required.

Finally, I must express my very profound gratitude to my parents, my younger brother Dip and to my husband Sanjoy Basak, for providing me with unfailing support and continuous encouragement throughout my years of study and through the process of researching and writing this thesis. This accomplishment would not have been possible without them.

ABSTRACT

The purpose of this study is to understand the electrospinning behaviour of cellulose acetate (CA) in different solvents and its subsequent modification and functionalization with polyethylene glycol (PEG) and silver nitrate (AgNO_3) to render it as a potential wound dressing material. As the process of electrospinning and the corresponding fibre properties are primarily governed by the solvents used, a systematic study of the selection of solvent systems using the solubility parameters of Hildebrand and Hansen along with a Teas chart for a particular polymer is essential for the better optimization of the process. It appeared from the Teas chart that higher dispersion force (f_d) and lower hydrogen bonding force (f_h) are convenient for both the solubility and spinnability of CA in single solvent of acetone and binary solvent of 2:1 acetone/N,N - dimethylacetamide (DMAc). The surface properties of CA fibres were roughened by adding PEG which improved swelling behaviour and would assist in rapid cell attachment during wound healing. Moreover, the presence of PEG stabilized the silver nanoparticles which displayed efficient antibacterial traits when tested against *E.coli* and *S.aureus*.

1. INTRODUCTION

1.1 Background and Research Significance

Electrospinning prevails for few decades as a facile method for weaving fibre meshes out of a solution. This technique offers some unique advantages along with the fact that the construction of this setup is remarkably economical and the operation is very convenient producing fibres in the nanometer range. Electrospinning from polymer solution is commonly in practice as polymer fibers are biocompatible and biodegradable and hence suitable for biomedical applications. Polymer fibers of nanometer range possess larger surface areas per unit mass and permit easier incorporation of surface functionalities compared with polymer microfibers. Thus, polymer nanofibers find their use as wound dressings, protective clothing, filters, scaffolds for tissue engineering reinforcement in composite materials, mirrors for use in space, structural components in artificial organs and sensors. These sophisticated applications of electrospun fibers have urged the need to address the electrospinning behavior for better process control [1-2].

Cellulose has been a potential choice of polymer in this regard for its renewability and easy availability and has a long history in fiber manufacturing. However, due to several challenges associated with cellulose solvents such as toxicity, low volatility and incomplete evaporation of the solvent, cellulose acetate which is the acetate ester of cellulose, is preferred for electrospinning. Cellulose acetate (CA) is readily soluble in a variety of solvents which makes it possible to study its electrospinning criteria for a number of solvent systems [3]. The opportunities of electrospun CA fibers lie in the fact that they are electrically charged. As a result, the fibers can be guided by electrical field for weaving, braiding, interlacing, coiling and similar operations. CA has not been widely explored for electrospinning in terms of solvents. There is a scope to study the electrospinning behavior of CA by analyzing its physio-chemical changes and the limitations of the process parameters to yield biocompatible and biodegradable fibers.

Chronic wounds are a worldwide healthcare problem. In case of any wounds, whether trivial or critical, a wound needs to be covered up with an external support to prevent infection. Thus, suitable wound dressing materials with ideal antimicrobial attributes are required to accelerate the healing process and restore the normal integrity of the body. This is why, there has been a boost in research focused on fabricating nanofibrous mats

having architectural features and morphological similarities with the natural extracellular matrix for better cell attachment and proliferation [4-6].

1.2 Objectives of the Present Study

Although electrospinning has been widely used in the world to yield nanofibers for various applications, to the best of the knowledge, no research on this technique has been conducted in Bangladesh till date. Thus, electrospinning has been attempted in this work with the following objectives:

- a. Electrospinning CA nanofibres by studying and optimizing process and solution parameters to fabricate beadless fibrous network
- b. Modifying surface morphology of CA fibres with PEG and studying the effect of PEG on swelling characteristics of the fibre
- c. Finally, functionalizing the electrospun fibres with AgNO₃ to produce in-situ Ag nanoparticles adhered to the fibre surface and study their antibacterial properties against gram negative and gram positive bacteria to establish this CA fibre as a potential wound dressing material.

1.3 Organization of the Thesis

The report has been organized so as to best describe and discuss the problem along with findings that came out from the experiment performed. Chapter 1 introduces the work and the technique which presents an overall idea about the research background and objectives of the study. Chapter 2 is literature review which represents the work performed so far in connection with it collected from different references. Chapter 3 presents the materials required and experimental setup used in the present study. This chapter presents the mechanism of electrospinning, different parameters that were tried to obtain suitable electrospinning conditions and the procedures of modifying and functionalizing the fibres with different chemical reagents. Chapter 4 begins the core of this thesis write up, which describes the individual materials required, characterizations performed, experimental results and explanations for obtaining CA fibre using electrospinning. It also established a correlation between solubility and spinnability of CA in different solvent systems using a Teas chart. Chapter 5, which is the continuation of the last chapter's work, describes the modification of the previously obtained fibre with PEG 200 and PEG 6000 with appropriate characterizations and discussions on the perceived results. Chapter 6 elaborates the functionalization of the modified CA fibre of the previous chapter to incorporate antibacterial properties in it. This chapter expounds on the method adopted to grow bacterial colonies on agar plate and subsequent testing of the fibre samples to show its efficacy in preventing bacterial growth. And, chapter 7 concluded the results that are obtained in this present study along with few recommendations on future work regarding electrospinning of CA.

2. LITERATURE REVIEW

2.1 Electrospinning

Electrospinning is a method to yield fibres using an electrical driving force and not by any mechanical force. Electrospinning is a process in practice for centuries which is able to fabricate continuous fibres in the submicron to the nanometer diameter range from a solution. Compared to the traditional techniques, the non-woven nanofibrous mats obtained by this process mimics extracellular matrix components more suitably. The wide range spun fibres, from micro to nano, produced by this process, offer various advantages like high surface area to volume ratio, tunable porosity and the ability to control nanofibre composition in order to get desired features and functions. This process is highly flexible as it can spin fibres from a broad range of material class. Though polymer solutions are more commonly used for electrospinning, it can be also possible to draw fibres with composites, semiconductors and ceramics [1-2]. Over the time, more than 200 polymers have been electrospun for myriad applications and the number is still escalating gradually with time. Fibre production is also viable through other production processes such as template synthesis, phase separation and drawing but owing to limitations of each of this methods, electrospinning has emerged as the most facile and cost-effective method of producing fibres.

2.1.1 History of electrospinning

Electrospinning is a time-old technique. It was first brought to attention in 1897 by Rayleigh, studied elaborately by Zeleny (1914) on electro spraying, and patented by Formhals in 1934. The work of Taylor (1969) on electrically driven jets has basically laid the foundation for electrospinning. Though the term “electrospinning”, derived from “electro- static spinning”, has been used relatively recently (in around 1994), its origin dated back to more than 70 years ago. This method started to gain attention, from 1934 to 1944, when Formhals published a series of patents, delineating an experimental setup for the production of polymer filaments using an electric field [3]. The first patent (US Patent Number: 2116942) on electrospinning was acknowledged for the fabrication of textile yarns where a voltage of 57 kV was used for electrospinning cellulose acetate using acetone and monomethyl ether of ethylene glycol as solvents. This process was

patented by Antonin Formhals in 1934 and also later granted related patents (U.S. Patents 2116942, 2160962 and 2187306) in 1938, 1939, and 1940 [4]. Formhals's spinning set-up consisted of a movable fibre collecting device to collect fibres in a stretched condition, like that of a rotating drum in conventional spinning. About 50 patents for electrospinning polymer melts and solutions have been filed in the past 70 years [5]. Vonnegut and Newbauer (1952) invented a simple apparatus for electrical atomization of solution and subsequently produced jets of highly electrified uniform droplets of about 0.1 mm in diameter. After that, Drozin (1955) investigated the spraying and dispersion of a series of liquids into aerosols under high electric fields and Simons (1966) patented an apparatus for the production of ultra-thin and very light weight non-woven fabrics with different patterns using electrical spinning. In 1971, Baumgarten (1971) made an apparatus to electrospin acrylic fibres with diameters in the range of 0.05– 1.1 μm . Since the 1980s and especially in recent years, electrospinning process has regained more attention due to a surging interest in nanotechnology, as ultrafine fibres or fibrous structures of various polymers with diameters down to submicrons or nanometers can be easily fabricated with this process [6]. The popularity of the electrospinning process can be realized by the fact that over 200 universities and research institutes worldwide are studying various aspects of the electrospinning process and the fibre it produces and also the number of patents for applications based on electrospinning has grown in recent years.

2.1.2 Electrospinning fundamentals

The formation of nanofibres through electrospinning has a well-grounded base on the uniaxial stretching of a viscoelastic solution. The principles of electrospinning and the different parameters that affect the process have to be considered to understand and appreciate the process that facilitates the formation of various nanofibre assemblies. In contrast to the conventional fibre spinning methods like dry-spinning and melt-spinning, electrostatic forces are utilized here in electrospinning to stretch the polymer solution as it solidifies. Similar to conventional fibre production methods, the drawing of the solution jet to form the fibre will continue as long as there is plenty of solution to feed the electrospinning jet. Thus, without any impediment to the electrospinning jet the drawing of the fibre will be continuous. For a typical electrospinning set-up as shown in Fig. 2.1, a polymer solution is first taken into a syringe and fed through a spinneret. An external high voltage is applied to the solution such that at a critical voltage, typically

more than 10 kV, the repulsive force within the charged solution is higher than its surface tension and a jet would initiate from the tip of the syringe. Although the jet is stable near to the tip of the syringe, a bending instability stage is observed with further stretching of the solution jet under the influence of the electrostatic forces in the solution as the solvent gradually evaporates. Generally, a grounded object is used to collect the resultant fibres which are deposited in the form of a nonwoven mesh [7-9]. A few widely studied electrospinning parameters include solution viscosity, conductivity, flow rate, applied voltage, spinneret tip-to-collector distance, temperature and humidity. For example, by reducing the spinneret tip-to-collector distance, mat with interconnected fibres can be obtained, while decreasing the solution concentration will reduce the diameters of the electrospun fibre. Although polymer chain entanglement is a vital criterion for fibre formation in polymers [10], the viscosity of a solution is a more general and tedious parameter to consider since ceramic precursors can also be electrospun in spite of their low molecular weight. There are usually two main methods to achieve various fibre morphologies, one is to control the flow of the electrospinning jet through the adjustment of the electric field and the other is to use a dynamic collection device. Nevertheless, it is also possible to achieve some form of fibre assemblies by using different static collection devices. To overcome various drawbacks of the typical electrospinning process and to enhance the performance of the electrospun fibrous mesh, researchers have brought out other modifications to the set-up.

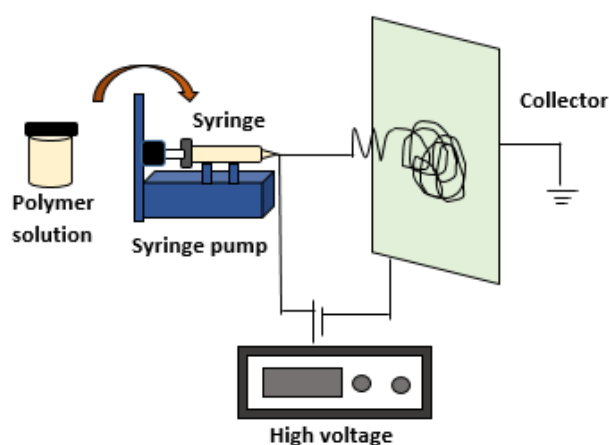


Fig. 2.1 Schematic setup of electrospinning

2.1.3 Electrospinning parameter investigation

There are quite a good number of parameters that can influence the transformation of polymer solutions into nanofibres through electrospinning. These parameters include (a) the solution properties such as viscosity, elasticity, conductivity, and surface tension, (b) governing variables such as hydrostatic pressure in the capillary tube, electric potential at the needle tip, and the gap (distance between the tip and the collecting screen), and (c) ambient parameters such as solution temperature, humidity, and velocity of the air in the electrospinning chamber [11].

Thus far, all synthetic and naturally occurring polymers have been electrospun. During selection of solvents for electrospinning, its properties such as solubility, conductivity, surface tension, and dielectric constant has to be taken into consideration. The molecular weight of the polymer has a tremendous effect on determining the fibre morphology. A high molecular weight results in a large fibre diameter, and a low molecular weight results in a beaded structure, which are considered defects in fibre formation. The viscosity of a polymeric solution significantly affects the fibre diameter. High viscosity more likely suppress the formation of pores, micropores, and beaded structures during electrospinning. If the viscosity is too low, the initiating jet from the Taylor cone will be transformed into many droplets, and the jet will experience splashing, thus resulting in beaded structure. If the viscosity is too high, then the viscoelastic forces will be high. As a result, a higher electrostatic force is required to overcome the viscoelastic forces and the jet will transformed into droplets instead of forming fibres. If the viscosity is above 20 poise, then electrospinning becomes impossible because of the instability of the flow caused by the cohesivity of the solution. Droplets are formed when the viscosity is low (<1 poise). A higher electrical conductivity can have significant influence on fibre diameter. In general, small-diameter fibres can be produced with a higher electrical conductivity solution. By reducing the surface tension of the polymeric solution, the fibres produced will be without beaded structures. Different solvents will result in different surface tension. However, a solvent with low surface tension is not always suitable for electrospinning because a solution with low surface tension helps electrospinning to occur at a low electrostatic field. The

viscosity of the polymeric solution and the diameter of the electrospun fibre are related by the following equation [12]:

$$d = 19.49 \eta^{0.43} \quad (1)$$

where η is the viscosity of solution and d is the diameter of the fibre (nm).

During the jet's flight from the tip of the needle to the collector screen, it experiences plastic stretching and evaporation due to natural convection, and as a result, the jet diameter gets smaller before it is collected on the collector screen. A higher electric field results in low fibre diameter, and these two parameters are related by the following equation [13],

$$d = V^{-1/2} \quad (2)$$

where V is the electrical potential. Hendricks calculated the minimum spraying potential of a suspended hemispherical conducting drop in air as

$$V = 300 \sqrt{(20\pi\gamma r)} \quad (3)$$

where r is the radius of the cone, and γ is the surface tension of the polymeric solution.

Taylor developed a similar relation for the critical potential as

$$V_c^2 = 4H^2/L^2 (\ln 2L/R - 3/2)(0.117\pi\gamma R) \quad (4)$$

where V_c is the critical voltage, H is the separation between the capillary and the ground, L is the length of the capillary, R is the radius of the capillary, and γ is the surface tension of the liquid.

The surface features and morphology of electrospun fibres depends upon flow rate of the solution. When the flow rate exceeds the threshold value, the fibres produced are surrounded by beads and pores. The polymer concentration is dependent upon the molecular weight of the polymer. However, concentration can be reduced by increasing the solvent content. The polymer concentration should not be too low or too high, but rather a compromise between maximum and minimum. The fibre diameter increases as the polymer concentration increases. If the polymer concentration is too high, then electrospinning becomes relatively difficult, and a higher electric field would be required to overcome the viscoelastic forces, or pores, micropores, and beads will form. Polymers with higher molecular have high viscosity in solution form and the resulting electrospun fibres will have large diameters. Molecular weight also greatly influences

the rheological properties of the polymeric solution. It has been observed that a low molecular weight solution produces beads and pores due to the low concentration of the solution, and a higher molecular weight solution produces fibres with large diameters due to the high concentration of the solution. The distance between the capillary tube and the collector screen also influences the fibre diameter: a large distance ensures enough time for the jet to undergo plastic stretching resulting in finer fibres. Generally, electrospinning process takes place at room temperature. At high temperature, the evaporation rate will be high, and thereby fibres having large diameters will be produced. High relative humidity during electrospinning leads to the formation of micropores and nanopores on the surface of the fibres due to the breath figures effect. Quick evaporation of the solvent condenses the moisture present in the air, leaving imprints in the form of micro- and nanopores on the surface of fibres. Some polymers absorb moisture and some do not, therefore, high humidity can decrease or increase the fibre diameter depending upon the polymer used. The presence of moisture in the electro- spinning chamber impedes evaporation. High airflow results in a higher evaporation rate, thus resulting in larger diameter fibres [14].

2.1.4 Applications of electrospinning

From a biological point of view, almost all of the human tissues and organs are arranged in nanofibrous forms or structures. Examples include: bone, dentin, collagen, cartilage, and skin. All of them are well-organized hierarchical fibrous structures aligned in nanometer scale. As such, current research in electrospun polymer nanofibres has focused one of their major applications on bioengineering. We can easily find their promising potential in various biomedical areas. Polymer nanofibres can be used for the treatment of wounds or burns of a human skin as shown in Fig. 2.2, as well as designed for haemostatic devices with some unique characteristics. With the aid of electric field, fine fibres of bio-degradable polymers can be directly sprayed onto the injured location of skin to form a fibrous mat dressing, which can let wounds heal by encouraging the formation of normal skin growth and eliminate the formation of scar tissue which would occur in a traditional treatment [15]. Non-woven nanofibrous membrane mats for wound dressing usually have pore sizes ranging from 500 nm to 1 mm which is small enough to protect the wound from bacterial penetration via aerosol particle capturing mechanisms. High surface area of 5–100 m²/g is extremely efficient for fluid absorption and dermal delivery [16].



Fig. 2.2 Nanofibre mat for wound dressing (www.boneandspine.com)

An important concern in medicine is to deliver drug/pharmaceuticals to patients in the most physiologically acceptable manner. In general, the drug is better absorbed by the human body when the dimensions of the drug and the coating material required to encapsulate the drug are smaller. Drug delivery with polymer nanofibres is based on the principle that dissolution rate of a particulate drug increases with increasing surface area of both the drug and the corresponding carrier if needed. Kenawy et al. investigated delivery of tetracycline hydrochloride based on the fibrous delivery matrices of poly (ethylene-co-vinylacetate), poly(lactic acid), and their blend [17]. Ignatious & Baldoni elaborated electrospun polymer nanofibres for pharmaceutical applications, which can be designed to provide rapid, immediate, delayed, or modified dissolution, such as sustained and/or pulsatile release characteristics. As the drug and carrier materials can be mixed together for electrospinning of nanofibres, the likely modes of the drug in the resulting nanostructured products are: (1) drug as particles attached to the surface of the carrier which is in the form of nanofibres, (2) both drug and carrier are nanofibre-form, hence the end product will be the two kinds of nanofibres intermixed together, (3) the blend of drug and carrier materials integrated into one kind of fibres containing both components, and (4) the carrier material is electrospun into a tubular form in which the drug particles are encapsulated as in Fig. 2.3. The modes (3) and (4) may be preferred. However, as the drug delivery in the form of nanofibres is still in the rudimentary stage exploration, a real delivery mode after production and efficiency have yet to be determined in the future [4][18].

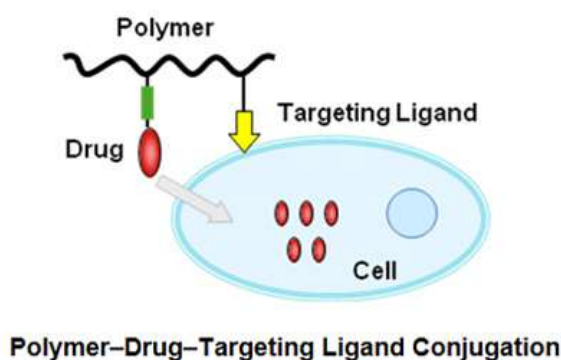


Fig. 2.3 Drug delivery through polymer nanofibre (www.dalton.com)

Conductive nanofibres have an excellent application in which they are expected to be used in the fabrication of tiny electronic devices or machines such as Schottky junctions, sensors and actuators. As it is a well-known fact that the rate of electrochemical reactions is proportional to the surface area of the electrode, conductive nanofibrous membranes are also quite suitable for using as porous electrode in developing high performance battery [19]. Conductive (in terms of electrical, ionic and photoelectric) membranes also have potential for applications including electrostatic dissipation, corrosion protection, electromagnetic interference shielding, photovoltaic device, etc [6][20].

Polymer nanofibres fabricated via electrospinning have been proposed for a number of soft tissue prostheses applications such as blood vessel, vascular, breast, etc as shown in Fig. 2.4. In addition, electrospun biocompatible polymer nanofibres can also be deposited as a thin porous film onto a hard tissue prosthetic device designed to be implanted into the human body. This coating film with gradient fibrous structure works as an interphase between the prosthetic device and the host tissues, and is expected to efficiently reduce the stiffness mismatch at the tissue/device interphase and hence prevent the device failure after the implantation [21].



Fig. 2.4 Artificial blood vessel (www.bioengineer.org)

Fibrous materials used for filter media come with the advantages of high filtration efficiency and low air resistance. In the industry, clean compressed air is produced by studying coalescing filter media. These media are required to capture oil droplets as small as 0.3 micron. It is realized that electrospinning is rising to the challenge of providing solutions for the removal of unfriendly particles in such submicron range. Since the channels and structural elements of a filter must be matched to the scale of the particles or droplets that are to be captured in the filter, one direct way of developing high efficient and effective filter media is by using nanometer sized fibres in the filter structure. In general, due to the very high surface area to volume ratio and resulting high surface cohesion, tiny particles of the order of <0.5 μm can be easily trapped in the electrospun nanofibrous structured filters and hence the filtration efficiency can be improved. There is one major manufacturer of electrospun products in the world, Freudenberg Nonwovens, which has been producing electrospun filter media from a continuous web feed for ultra high efficiency filtration markets for more than 20 years. This is perhaps one of the earliest commercial businesses relevant to electrospinning. In addition to fulfilling the more conventional purpose in filtration, the nanofibre membranes fabricated from some specific polymers or coated with some selective agents can also be used as, for example, molecular filters. For instance, such filters can be applied to the detection and filtration of chemical and biological weapon agents [22-23].

Like other 1D nanostructures, electrospun nanofibres can also serve as sacrificial templates to generate 1D nanostructures with hollow interiors. A range of polymers, metals, and ceramics have been prepared as nanotubes by coating electrospun polymer nanofibres with the particular material, followed by selective removal of the templates.

Most recently, Czaplewski et al. have demonstrated that electrospun fibres could be used as the templates to generate nano fluidic channels [24]. In this case, nanofibres made of heat depolymerizable polycarbonate were deposited on a target substrate and then covered with spin on glass. Nanofluidic channels were obtained after the nanofibres had been selectively removed by heating. Unlike the channels that were fabricated by conventional lithographic techniques, the channels obtained by templating against electrospun fibres exhibited elliptical cross-sections and sharp corners were eliminated. This structure may promote a smoother liquid flow through the channels. In conjunction with contact photolithography, they have also demonstrated the application of electrospun fibres as the templates for fabricating nanoscale mechanical oscillators. In these two applications, the size uniformity and long axial length associated with electrospun fibres provide some immediate advantages over conventionally fabricated structures [25-26].

2.2 Polymers Used In Electrospinning

Polymers comprise of a broad spectrum which can be electrospun into nonwoven fibres in the range of nano to submicron and has potential use in myriad fields. Various synthetic polymers, natural polymers or a blend of both including proteins and even polysaccharides have been reported to be electrospun [27-28]. Over the years, more than 200 polymers have been electrospun successfully from several natural polymers and characterized with respect to their applications. Compared to synthetic polymers, it has been evaluated that naturally occurring polymers normally exhibit better biocompatibility and low immunogenicity, when used in biomedical applications. A vital reason for using natural polymers for electrospinning is their inherent capability for binding cells since they carry specific protein sequences, such as RGD (arginine/glycine/ aspartic acid). Typical natural polymers include collagen, chitosan, gelatin, casein, cellulose acetate, silk protein, chitin, fibrinogen etc. Scaffolds synthesized from natural polymers yield better clinical functionality. However, partial denaturation of natural polymers has been reported in recent years that demands concern. Various polymers used in electrospinning and applications have been listed in Table 2.1.

Table 2.1: Different polymers used in electrospinning and their applications [28]

Polymers	Applications
Poly(glycolide) (PGA)	Nonwoven TE scaffolds
Poly(lactide-co-glycolide)(PLGA)	Biomedical applications, wound healing
Poly(ϵ -caprolactone) (PCL)	Bone tissue engineering
Poly(L-lactide) (PLLA)	3D cell substrate
Polyurethane (PU)	Nonwoven tissue template wound healing
Cellulose acetate	Adsorptive membranes/felt
Poly(vinyl alcohol)	Wound dressings
Silk fibroin, silk/PEO	Nanofibrous TE scaffold
Silk	Biomedical Applications
Silk fibroin	Nanofibrous scaffolds for wound healing
Gelatin	Scaffold for wound healing
Hyaluronic acid, (HA)	Medical implant
Cellulose	Affinity membrane
Collagen/chitosan	Biomaterials

2.3 Cellulose Acetate: A Potential Polymer in Electrospinning

CA has emerged as a lucrative polymer choice for electrospinning due to its wide range of behavior, property and application. CA is a valuable bio-based polymer which has been resulted from the esterification of cellulose. The acetylation of 2.5 hydroxyl groups of a monomeric unit of cellulose chain gives the typical 2.5 cellulose acetate (CA). It is sometimes called Acetylated cellulose or xylonite. Its CAS number is 9004-35-7 and the approximate chemical structure is shown in Fig. 2.5.

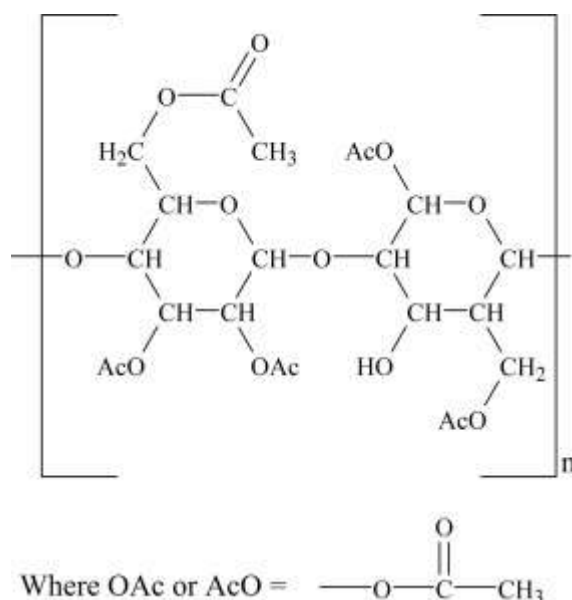


Fig. 2.5 Chemical structure of CA

CA is highly hydrophilic, with good water absorption and liquid transport abilities. CA, the acetate ester of cellulose, has been widely investigated for a wide variety of potential applications in the form of electrospun nanofibre mats because of its advantageous properties, such as good biocompatibility, biodegradability, regenerative properties, high affinity with other substances, high modulus, and adequate flexural and tensile strength [29]. These sophisticated properties have rendered CA to be effectively used in immobilization of bioactive substances, drug-loaded electrospun materials, cell-culture and tissue engineering, optical device, nanomaterials loaded antimicrobial mat, temperature adaptable fabrics and so on.

A central point of research over the years has been the selection of suitable solvent system for dissolving and electrospinning CA fibres. The selection of appropriate solvents has been conventionally based on trial and error, results from similar systems or solubility models restricted by physico-chemical database [30]. Some have reported the effect of various single and mixed solvent systems on the morphology and fibre diameter of CA [31]. The single solvent system comprised of acetone, chloroform, N, N-dimethylformamide (DMF), dichloromethane (DCM), formic acid, methanol (MeOH) and pyridine. Acetone–dimethylacetamide (DMAc), chloroform–MeOH, and DCM–MeOH were among the mixed or binary solvent systems. In generating bead free or beaded fibres, the shear viscosity, surface tension, and conductivity of these solvent systems have been evaluated to be critical solution parameters. Even ternary solvent

system of acetone/DMF/trifluoro-ethanol has also been determined for electrospinning cellulose acetate [32]. However, there are not many reports available on the influence of ambient parameters and electrospinning parameters on the nature of electrospun CA fibres. The average diameter of electrospun CA nanofibres was found to increase with increase in humidity. On the other hand, temperature influences the solvent evaporation rate and viscosity of the polymer solution. Both these parameters were found to have profound influence on the fibre diameter of electrospun CA [33]. The effect of different parameters including field strength, tip-to-collector distance, solution feed rate and composition on the morphology of electrospun CA fibres was reported in many literatures. A growing interest on the development of electrospun CA as blends and composites has been witnessed in the last few years (2008–2015). A myriad of natural and synthetic polymers and nanomaterials have been electrospun along with CA to generate more customized products. The applications of CA fibres have been demonstrated in the Fig. 2.6.

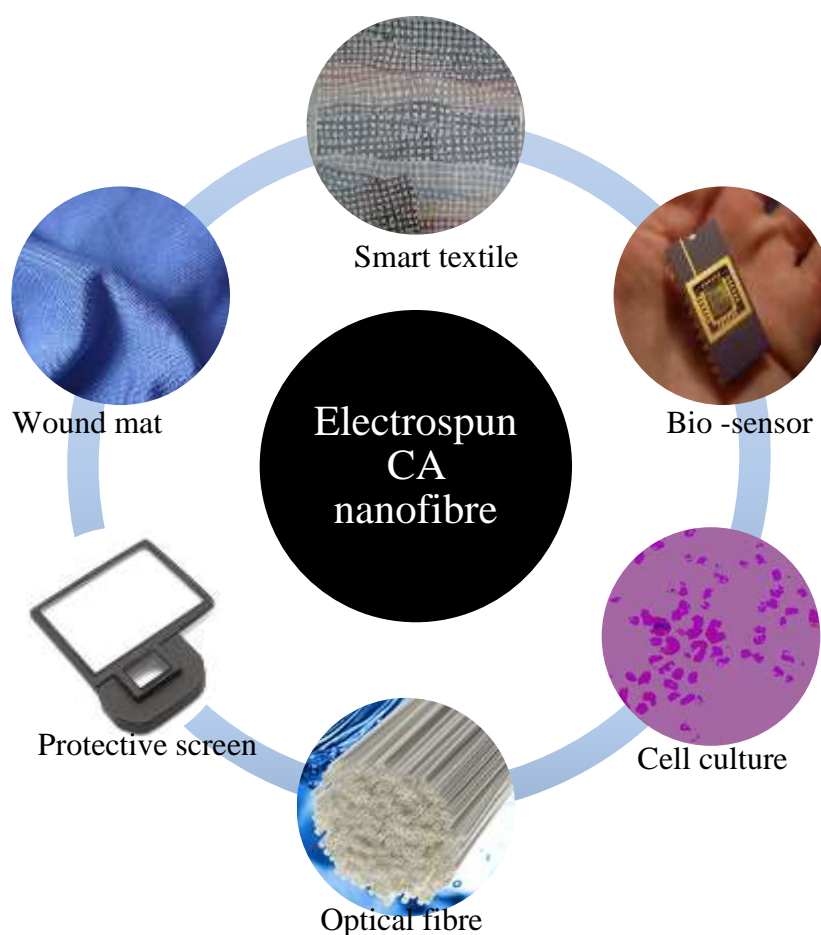


Fig. 2.6 Applications of CA fibres in different arena

2.4 Polyethylene Glycol

2.4.1 Polyethylene glycol as a modifier

Poly(ethylene glycol) (PEG), also called poly(ethylene oxide) (PEO) in its high molecular weight form, can be categorized as a hydrogel, especially when the chains are cross-linked. However, PEG has many other applications and implementations. In 1944, when it was examined as a possible vehicle for intravenously administering fat-soluble hormones, the low reactivity of PEG with living organisms has been known since then. In the mid-1970s, Frank Davis and colleagues discovered that if PEG chains were attached to enzymes and proteins, they would have a much longer functional residence time *in vivo* than biomolecules that were not PEGylated. Professor Edward Merrill of MIT, concluded that surface-immobilized PEG would resist protein and cell pickup. The experimental results from his research group in the early 1980s bore out this conclusion. The application of PEGs to wide range of biomedical problems was significantly accelerated by the synthetic chemistry developments of Dr. Milton Harris while at the University of Alabama, Huntsville.

PEG is readily available in a variety of molecular weights. These are homogeneous polymers of the general structure $\text{HO}-(\text{CH}_2\text{CH}_2\text{O})_n-\text{CH}_2\text{CH}_2-\text{OH}$. Monomethyl ether of PEG (mPEG) is also often used for conjugation to biologically relevant materials. It is particularly useful when multiple chains of the polymer have to be linked to the intended substrate. Due to its structural simplicity and possession of only one derivatizable end group, the use of mPEG minimizes crosslinking possibilities and leads to improved homogeneity of conjugates. Thus it is usually the starting material of choice for covalent modification of proteins, biomaterials, and particulates. The polyether backbone of PEG is inert in biological environments as well as in most chemical reaction conditions under which the end groups of PEG can be subjected to chemical modification and/or conjugation reactions [34].

Fabrication of micro- and nanosized fibres from biodegradable polymers, either natural or synthetic by electrospinning, is a great challenge because of their possible applications, including tissue engineering, tissue repair, wound healing, and drug delivery [35-36]. To augment the hydrophilicity of the electrospun fibres, a copolymer with a hydrophilic block has been added to the spinning solutions. Using this approach, CA-PEG fibres with enhanced hydrophilicity have been obtained in the present study.

PEGs of molecular weight lower than 6,000 are particularly suitable for this purpose. These PEGs are widely used in the biomedical field because of their unique properties, including lack of toxicity and good biocompatibility; in addition they are easily eliminated from the human body [37].

Recently, PEG has proved to be very effective in preventing bacterial adhesion to cell as well by forming a hydration layer [38]. To the best of our knowledge, PEGs have not yet been used to study swelling behaviour of electrospun fibre mats of CA polymers. The reason may be due to the difficulty to electrospin nanofibres from polymers of chain lengths that are too short for the formation of chain entanglements.

2.4.2 Polyethylene glycol as a stabilizer

For the synthesis of silver nanoparticles, the generally accepted mechanism suggests a two-step process, i.e. atom formation and then polymerization of the atoms. In the first step, a portion of metal ions in a solution is reduced by the available reducing groups. The atoms thus produced act as nucleation centers and catalyze the reduction of the remaining metal ions present in the bulk solution. Subsequently, the atoms coalesce leading to the formation of metal clusters. The surface ions are again reduced and in this way the aggregation process does not cease until high values of nuclearity are attained, which results in larger particles. The process is stabilized by the interaction with the polymer so preventing further coalescence [39].

It is important to use protective agents to stabilize dispersive nanoparticles during the course of metal nanoparticle preparation, and protect the nanoparticles that can be absorbed on or bind onto nanoparticle surfaces, avoiding their agglomeration [40]. The presence of surfactants comprising functionalities (e.g., thiols, amines, acids, and alcohols) for interactions with particle surfaces can stabilize particle growth, and protect particles from sedimentation, agglomeration, or losing their surface properties. Metal clusters formed at the interface are stabilized, due to their surface being coated with stabilizer molecules occurring in the non-polar aqueous medium, and transferred to the organic medium by the inter-phase transporter. PEG also acts as a good stabilizer for Ag nanoparticles based on the conclusions made by several research studies as mentioned in several works. The large number of oxygens in the long PEG chains provided coordinative saturation of dangling bonds on the surface of the nanoparticles and hence assisted in their stabilization, even though the electron-donating effect of oxygen is not

so strong as amine or thio-organic compounds. The researchers suggested that stabilization can be obtained due to the free polymer chains in solution, where formation of aggregates is denied because of steric hindrance. From their observation, they also proposed that increasing the molecular weight of the polymer would help in forming stable Ag nanoparticles [41-44].

2.5 Wound Dressings

2.5.1 Traditional wound dressing

Notable and some common traditional wound dressing products consist of gauze, lint, plasters, bandages (natural or synthetic) and cotton wool. These are dry and protect the wound from contaminations by acting as either primary or secondary wound dressings. Gauze dressings are made out of woven and non woven fibres of cotton, rayon, polyesters which provide some extent of protection against microbial infections. While some sterile gauze pads are used for absorbing exudates and fluid in an open wound with the help of fibres in these dressings. However, these dressings require frequent changing to protect from exaggeration of healthy tissues. Gauze dressings are less cost effective. Due to excessive wound exudates formation, dressings become moistened and tend to become adherent to the wound making it painful when removing. Natural product b such as those made from natural cotton wool and cellulose or synthetic bandages made out of polyamide materials carry out different functions. For instance, cotton bandages are used for applying light dressings, whereas high compression bandages and short stretch compression bandages provide sustained compression in case of venous ulcers. Xeroform™ (non-occlusive dressing) is petrolatum gauze with 3% of Bismuth tribromophenate used for non-exudating to slight exudating wounds. Tulle dressings such as Bactigras, Jelonet, Paratulle are some examples of tulle dressings commercially available as impregnated dressings with paraffin and suitable for superficial clean wound. Generally traditional dressings are indicated for the clean and dry wounds with mild exudate levels or used as secondary dressings. Since traditional dressings fail to provide moist environment to the wound they have been replaced by modern dressings with more advanced formulations [45].

2.5.2 Modern wound dressing

Modern wound dressing have been a boon to improve the function of the wound rather than just to cover it. These dressings are focused to prevent the wound from dehydration

and facilitate healing. Based on the cause and type of wound, numerous products are available in the market. Modern wound dressings are usually based on synthetic polymers and are classified as passive, interactive and bioactive products. Passive products are non-occlusive, such as gauze and tulle dressings, used to cover the wound to restore its function underneath. Interactive dressings are semi-occlusive or occlusive, available in the forms of films, foam, hydrogel and hydrocolloids. These dressings act as a barrier against penetration of bacteria to the wound environment [46-47].

2.5.3 Electrospun fibres as wound dressing

The wound dressing materials produced by electrospinning technology have special properties as compared to the dressings produced by conventional methods. Nanofibrous wound dressings with their small holes and high effective surface area can promote hemostasis phase. The promotion of this phase is due to nanofibrous structure of the dressing material without using any hemostatic agent. Due to the high surface area to volume ratio of the nanofibres, they exhibit water absorption of 17.9–213% whereas typical film dressings only show water absorption of 2.3%. Thus, if hydrophilic polymers are employed, the nanofibrous dressings will be able to absorb wound exudates more efficiently than the typical film dressings. The porous structure of a nanofibre dressing is excellent for the respiration of cells which does not lead the wound to dry up. This indicates an appropriate control of a moist environment for the wound. Also, the small pore size can effectively protect the wound from bacterial infection. Electrospun nanofibrous membrane wound dressings can also meet the requirement of high gas permeation apart from providing effective protection of wound against infection and dehydration. Conformability or the ability to conform to the contour of wound is one of the parameters that needs to be clinically assessed for the flexibility and resiliency of the medical dressings. In the textile industry, it is widely recognized that the conformability of a fabric is closely related to the fibre fineness. Finer fibre fabrics are easier to fit to complicated 3-D contours. Therefore, dressing materials made of ultra-fine fibres can provide excellent conformability and thus result in a better coverage and protection of the wounds from infection. Ultimately, nanofibres also hold a promise of healing wounds without leaving scars. Although this is hard to achieve, nevertheless researchers and clinicians seek to heal a wound with as little scar as possible [48-49].

2.6 Silver: An Antibacterial Agent In Electrospun Fibre Mat

The broad-spectrum antimicrobial properties of silver incite its use in biomedical applications, water and air purification, food production, cosmetics, clothing, and numerous household products. With the rapid development of nanotechnology, applications have been extended further and now silver is the engineered nanomaterial most commonly used in consumer products. Clothing, respirators, household water filters, antibacterial sprays, cosmetics, detergent, dietary supplements, cutting boards, sox, shoes, cell phones, laptop keyboards, and children's toys are among the retail products that increasingly exploit the antimicrobial properties of silver nanomaterials. Different forms of silver nanomaterials already in such products include: metallic silver nanoparticles, silver chloride particles, silver-impregnated zeolite powders and activated carbon materials, dendrimer-silver complexes and composites, polymer silver nanoparticle composites and silver nanoparticles coated onto polymers like polyurethane. While all of these forms of silver exert antimicrobial activity to some extent through release of silver ions, silver nanoparticles might exhibit additional antimicrobial capabilities not exerted by bulk or ionic silver. Table 2.2 presents a concise summary of silver nanomaterial antibacterial studies.

Table 2.2: Summary of Ag nanoparticles in antibacterial study

Ag form	Size	Bacterial strain	Key aspects	References
Ag nanoparticles	13.4 nm	E. coli, S. aureus	Minimal inhibition concentration against E. coli was lower than 6.6 nM and higher than 33 nM for S. aureus	[50]
Ag nanoparticles applied as aerosol	16 nm	E. coli	Complete inhibition of CFU ability at 60 lg/mL	[51]
	1 μ m	E. coli, S. aureus	CFU reduced by 4 to 5 log units	[52]
	26 nm	Standard strains and strains isolated from clinical material	Minimal inhibition concentration from 1.69 to 13.5 lg/mL	[53]
	10 nm	E. coli, S. aureus, L. mesenteroides	Growth inhibition achieved at 5 lg/mL	[54]
Silver nanoparticles stabilized in hyperbranched polymers	14.1-710 nm	B. subtilis, K. mobilis	76% CFU reduction by applying silver nanoparticles aerosol on B. subtilis aerosol	[55]
Silver–dendrimer complexes and nanocomposites	1.4-7.1 nm	E. coli, S. aureus, B. subtilis, K. mobilis	Microbial activity increases as silver content in polymer decreases since decrease in silver nanoparticle size	[56]

2.6.1 Synthesis routes of silver nanoparticles

Silver nanoparticles have received considerable attention due to their attractive physical and chemical properties. Metallic silver colloids were first prepared more than a century ago. Ag nanoparticles can be synthesized using various methods: chemical, electrochemical, γ -radiation photochemical, laser ablation etc [57-58].

In physical processes, metal nanoparticles are generally synthesized by evaporation–condensation, which could be carried out using a tube furnace at atmospheric pressure. The source material within a boat centered at the furnace is vaporized into a carrier gas. Nanoparticles of various materials, such as Ag, Au, PbS and fullerene, have previously been produced using the evaporation/condensation technique [59-60]. However, the generation of Ag nanoparticles using a tube furnace has several drawbacks, because a tube furnace occupies a large space, consumes a great deal of energy while raising the environmental temperature around the source material, and requires a lot of time to achieve thermal stability. A typical tube furnace requires power consumption of more than several kilowatts and a preheating time of several tens of minutes to attain a stable operating temperature.

Ag nanoparticles were synthesized via a small ceramic heater that has a local heating area. Because the temperature gradient in the vicinity of the heater surface is very steep in comparison with that of a tube furnace, the evaporated vapor can cool at a suitably rapid rate. This makes possible the synthesis of small nanoparticles in high concentration. This method might be suitable for a variety of applications, including utilization as a nanoparticle generator for long-term experiments for inhalation toxicity study and as a calibration device for nanoparticle measurement equipment [61].

Moreover, Ag nanoparticles have been synthesized with laser ablation of metallic bulk materials in solution [62-63]. The characteristics of the metal particles formed and the ablation efficiency strongly depend upon many parameters such as the wavelength of the laser impinging the metallic target, the duration of the laser pulses (in the femto-, pico- and nanosecond regime), the laser fluence, the ablation time duration and the effective liquid medium, with or without the presence of surfactants [64-65].

The laser fluence is one of the most important parameters. Indeed, the ejection of metal particles from the target requires a minimum power. The mean size of the nanoparticles has been found generally to increase with increasing laser fluence and is generally smallest for fluencies not too far above the laser breakdown threshold. Besides the laser fluence, the number of laser shots (i.e. the time spent during laser vaporization) influences the concentration and the morphology of metal particles released in a liquid. For longer times under the laser beam the metal particle concentration is expected to increase, but it can saturate due to light absorption in the colloid highly concentrated in metal particles.

Moreover, nanoparticles can be modified in size and shape due to their further interaction with the laser light passing through [66]. Also, the formation of nanoparticles by laser ablation is terminated by the surfactant coating. The nanoparticles formed in a solution of high surfactant concentration are smaller than those formed in a solution of low surfactant concentration.

One advantage of laser ablation compared to other conventional method for preparing metal colloids is the absence of chemical reagents in solutions. Therefore, pure colloids, which will be useful for further applications can be produced by this method [67].

Chemical reduction is the most frequently applied method for the preparation of AgNPs as stable, colloidal dispersions in water or organic solvents. Commonly used reductants are borohydride, citrate, ascorbate and elemental hydrogen. The reduction of silver ions (Ag^+) in aqueous solution generally yields colloidal silver with particle diameters of several nanometers. Initially, the reduction of various complexes with Ag^+ ions leads to the formation of silver atoms (Ag^0), which is followed by agglomeration into oligomeric clusters. These clusters eventually lead to the formation of colloidal Ag particles [68-69].

Previous studies showed that use of a strong reductant such as borohydride, resulted in small particles that were somewhat monodispersed, but the generation of larger particles was difficult to control. Use of a weaker reductant such as citrate, resulted in a slower reduction rate, but the size distribution was far from narrow [70].

It is important to use protective agents to stabilize dispersive nanoparticles during the course of metal nanoparticle preparation. The most common strategy is to protect the

nanoparticles with protective agents that can be absorbed on or bind onto the nanoparticle surface, avoiding their agglomeration [71-72].

For instance, dodecanethiol-capped AgNPs, were prepared based on Brust procedure, that based on a phase transfer of an Au^{3+} complex from aqueous to organic solution in a two-phase liquid-liquid system, followed by a reduction with sodium borohydride in the presence of dodecanethiol as stabilization agent which bind onto the nanoparticles surface, avoiding their aggregation and making them soluble in certain solvents. They showed that small changes in synthetic parameters lead to dramatic modifications in nanoparticle structure, average size, size distribution width, stability and self-assembly patterns.

The most commonly used polymers for this purpose were poly(vinylpyrrolidone) (PVP), poly(ethylene glycol) (PEG), poly(methacrylic acid) (PMAA), polymethylmethacrylate (PMMA) and so on [73-74].

Also, Ag nanoparticles can be prepared inside microemulsion. The synthesis of Ag nanoparticles in two-phase aqueous organic systems is based on the initial spatial separation of reactants (metal precursor and reducing agent) in two immiscible phases. The rate of subsequent interaction between the metal precursor and the reducing agent is controlled by the interface between the two liquids and by the intensity of interphase transport between the aqueous and organic phases, which is mediated by a quaternary alkyl-ammonium salt. Metal clusters formed at the interface are stabilized, due to their surface being coated with stabilizer molecules occurring in the nonpolar aqueous medium, and transferred to the organic medium by the interphase transporter.

This method allows preparation of uniform and size controllable nanoparticles. However, a highly deleterious organic solvent is employed in this method. Thus large amounts of surfactant and organic solvent, which are added to the system, must be separated and removed from the final product. As a result, it is expensive to fabricate silver nanoparticles by this method [75].

On other hand, the advantages of forming particles which are readily dispersed in organic media are recognized by scientific workers in many fields. For example, colloidal nanoparticles prepared in nonaqueous media for conductive inks are well-dispersed in a low vapor pressure organic solvent, to readily wet the surface of polymeric substrate without any aggregation. The advantages can also be found in the

applications of nanometal particles as catalysts to catalyze most organic reactions, which take place in nonpolar solvents. It is very important to transfer nanoparticles to different chemico-physical environments in the practical applications. Ag nanoparticles were produced via photoreduction of AgNO_3 in layered inorganic clay suspensions, which serves as stabilizing agent that prevent nanoparticles from aggregation. The properties of silver nanoparticles were studied as a function of the UV irradiation time. A bimodal size distribution and relatively large silver nanoparticles were obtained when irradiated under UV for 3 h. Further irradiation disintegrated the Ag nanoparticles into smaller size with a single mode distribution until a relatively stable size and size distribution were achieved [76].

Recently, biosynthetic methods employing naturally occurring reducing agents such as polysaccharides, biological micro-organism such as bacteria and fungus or plants extract, i.e. green chemistry, have emerged as a simple and viable alternative to more complex chemical synthetic procedures to obtain Ag nanoparticles.

Three main steps, which must be evaluated based on green chemistry perspectives, including selection of solvent medium, selection of environmentally benign reducing agent, and selection of nontoxic substances for the silver nanoparticles stability. For instance starch Ag nanoparticles were prepared using starch as a capping agent and β -D-glucose as a reducing agent in a gently heated system. The starch in the solution mixture avoids use of relatively toxic organic solvents. Additionally, the binding interactions between starch and Ag nanoparticles are weak and can be reversible at higher temperatures, allowing separation of the synthesized particles [77-78].

Green tea (*Camellia sinensis*) was used extract as reducing and stabilizing agent to produce gold silver nanoparticles in aqueous solution at ambient conditions. Furthermore, the synthesis of Ag nanoparticles was reported by reduction of aqueous Ag^+ ions with the culture supernatant of *Bacillus licheniformis*. The synthesized Ag nanoparticles are highly stable and this method has advantages over other methods as the organism used here is a non-pathogenic bacterium [79-80].

2.6.2 Mechanisms of silver's antibacterial properties

Although the mechanisms behind the activity of nano-scaled silver on bacteria are not yet fully elucidated, the three most common mechanisms of toxicity proposed to date are: (1) uptake of free silver ions followed by disruption of ATP production and DNA

replication, (2) Ag nanoparticle and Ag ion generation of ROS, and (3) silver nanoparticle direct damage to cell membranes. The various observed and hypothesized interactions between silver nanomaterials and bacteria cells are conceptually illustrated in Fig. 2.7.

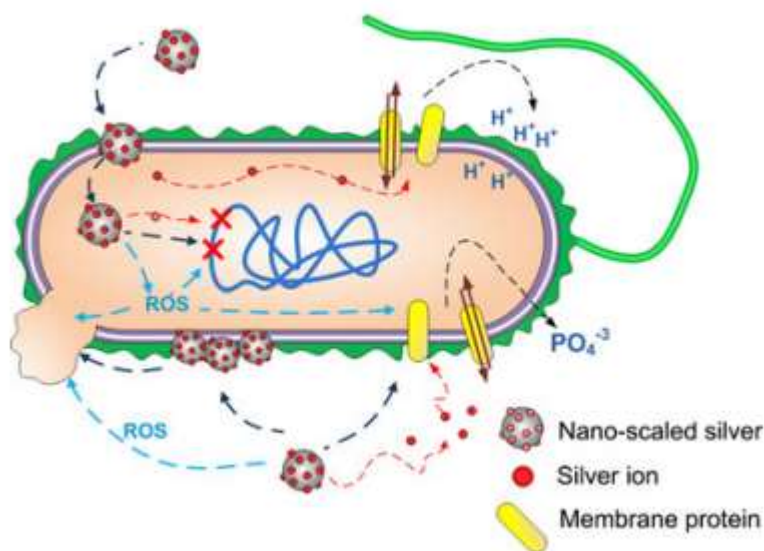


Fig. 2.7 Diagram summarizing nano-scaled silver interaction with bacterial cells.

Similar pictures have been published in [81]

Reactive oxygen species (ROS) are natural byproducts of the metabolism of respiring organisms. While small levels can be controlled by the antioxidant defences of the cells such glutathione/glutathione disulfide (GSH/GSSG) ratio, excess ROS production may produce oxidative stress [81]. The additional generation of free radicals can attack membrane lipids and lead to a breakdown of membrane and mitochondrial function or cause DNA damage [82]. Metals can act as catalysts and generate ROS in the presence of dissolved oxygen [83]. In this context, silver nanoparticles may catalyze reactions with oxygen leading to excess free radical production. Studies done in eukaryotic cells suggest that Ag nanoparticles inhibit the antioxidant defence by interacting directly with GSH, binding GSH reductase or other GSH maintenance enzymes [84]. This could decrease the GSH/GSSG ratio and, subsequently, increase ROS in the cell. Ag ions eluted from nano-scaled silver or chemisorbed on its surface may also be responsible for the generation of ROS by serving as electron acceptor. In bacterial cells, Ag ions would likely induce the generation of ROS by impairing the respiratory chain enzymes through direct interactions with thiol groups in these enzymes or the superoxide radical

scavenging enzymes such as superoxide dismutases [85]. Silver nanoparticles interact with the bacterial membrane and are able to penetrate inside the cell. Silver nanoparticle accumulation on the cell membrane and uptake within the cell has also been reported for other bacteria such as *V. cholera*, *P. aeruginosa*, and *S. typhus*. In these cases, only nanoparticles smaller than 10 nm attached to bacteria cell membranes or were observed inside the bacteria [86]. However, in other research Ag nanoparticles with sizes up to 80 nm were transported through the inner and outer membrane of *P. Aeruginosa* [87]. Ag nanoparticle composites and silver nanoparticles stabilized with surfactants are also thought to interact with cell membranes. The detailed mechanism by which Ag nanoparticles interact with cytoplasmic membranes and are able to penetrate inside cells is not fully determined. One hypothesis is that the interaction between nanoparticles and bacterial cells are due to electrostatic attraction between negatively charged cell membranes and positively charged nanoparticles [51].

3. EXPERIMENTAL OVERVIEW

The experimental work carried out in this study has been delineated here in this section along with materials used in different stages of this work.

3.1 Materials

Cellulose acetate, CA (acetyl content 39.8% and $M_n = 30,000$ by GPC) and AgNO_3 were acquired from Sigma-Aldrich. The solvents acetic acid (purity 100%), acetone (purity 100%) and N,N-Dimethylacetamide (DMAc) (purity 99%) were purchased from Merck. Polyethylene glycol (PEG) of molecular weight 200 and 6000 and citric acid (CT) monohydrate were also obtained from Merck.

3.2 Preparation of CA Solutions

CA solutions were prepared in three different solvent systems: 10, 12, 15, 17 and 19 wt% of CA in 3:1 acetic acid/water, 17 and 19 wt% of CA in 2:1 acetone/DMAc and 17 and 19 wt% of CA in pure acetone. A required quantity of CA was weighed and magnetically stirred with the solvents for 4-5 hrs at room temperature to obtain a clear solution. Fig. 3.1 showed the clear CA solution.



Fig. 3.1 Clear, viscous 17 wt% CA solution in 3:1 acetic acid/water stirred for 4 hrs

However, when water and 100% acetic acid were tried as a solvent for CA, CA did not dissolve and CA particles remained dispersed in the water even after stirring. Thus water and acetic acid proved to be a non-solvent for CA. Fig. 3.2 depicted the insolubility of CA in water and 100% acetic acid.

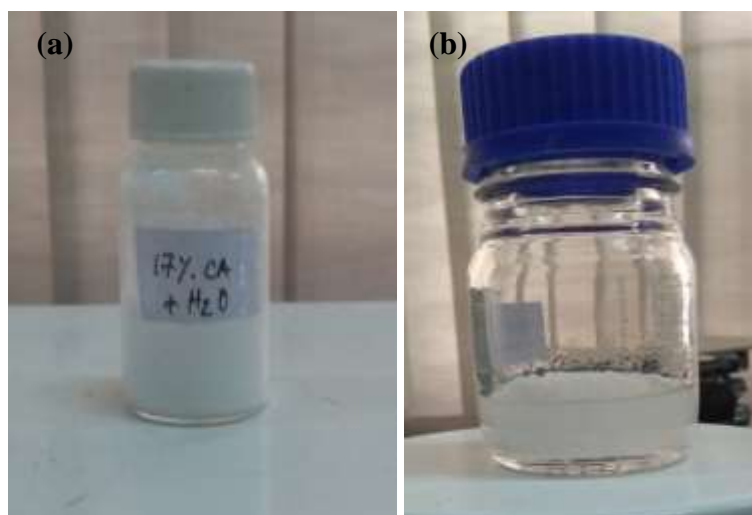


Fig. 3.2 17 wt% CA in (a) water and (b) 100% acetic acid

3.3 Preparation of CA Solutions with PEG and AgNO_3

In order to modify surface properties, the above solution of 17 wt% CA in 2:1 acetone/DMAc was further stirred with 10, 20, 40 and 80 wt% PEG-200 and 10 wt% PEG-6000 of CA. To this, 1 wt% AgNO_3 of CA was added and stirred. Upon stirring, the colour of the solution gradually changed from colourless to light yellow and then finally turned dark brown indicated in Fig. 3.3. This confirmed the reduction of AgNO_3 to Ag particles.

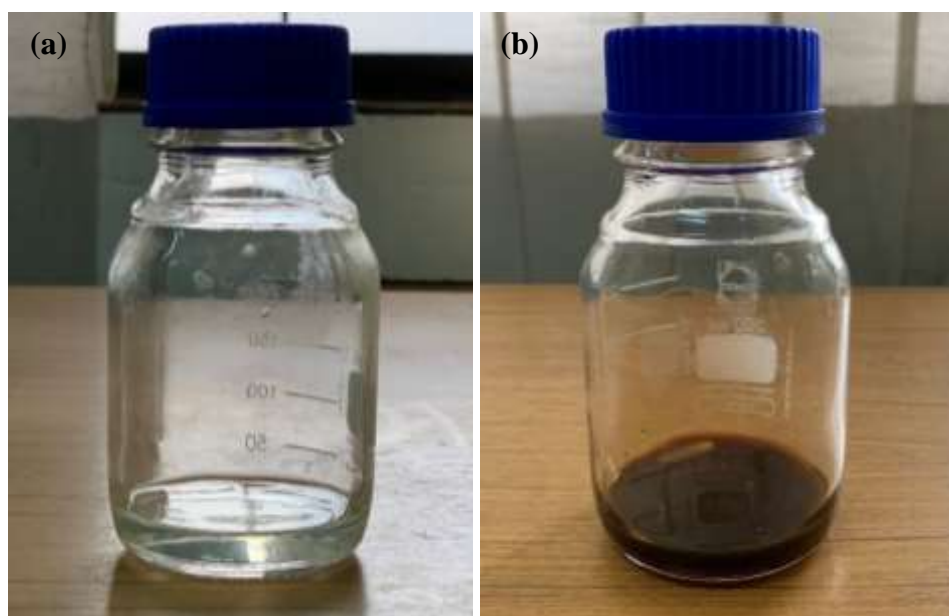


Fig. 3.3 CA solution in 2:1 acetone/DMAc (a) before and (b) after adding AgNO_3

3.4 Electrospinning of CA Solutions into Fibre

The as-prepared polymer solutions were electrospun through an in-house electrospinning setup. During electrospinning the process variables were selected based on literature review and initial experiments [88-89]. Voltages of 17, 20 and 25 kV and a feed rate of 0.5, 1.5 and 3 ml/h were employed for the CA solutions initially. Variation of electrospinning and solution parameters are showed in Table 3.1. A stable jet formed without clogging the needle tip and uniform fibres without beads were collected. Similar results have also been reported elsewhere [90]. The tip to collector distance was fixed at 10 cm. The electrospinning was carried out at room temperature. The collected fibre mats showed in Fig. 3.4 were dried overnight in an oven at 40°C. The following table accounted the trials that have been made by altering various factors to obtain fibre mat by electrospinning. A schematic of the electrospinning set-up and spinning was represented in Fig. 3.5.

Table 3.1: Variation of electrospinning and solution parameters to obtain fibre

Sample No.	Wt% of CA	Solvent	Flow rate (ml/hr)	Voltage (kV)	Distance (cm)	Observation
1	17	100 % water	3	20	10	No solution
2	17	100% acetic acid	3	20	10	No solution
3	17	75:25 acetic acid & water	3	20	10	Viscous solution forms
4	12	75:25 acetic acid & water	3	20	10	Viscous solution forms
5	10	75:25 acetic acid & water	3	20	10	Viscous solution forms
6	10	75:25 acetic acid & water	1.5	20	10	Viscous solution forms

Sample No.	Wt% of CA	Solvent	Flow rate (ml/hr)	Voltage (kV)	Distance (cm)	Observation
7	10	75:25 acetic acid & water	1.5	25	10	Viscous solution forms
8	15	75:25 acetic acid & water	1.5	20	10	Viscous solution forms
9	15	75:25 acetic acid & water	0.5	20	10	Viscous solution forms
10	17	75:25 acetic acid & water	1.5	20	10	Viscous solution forms
11	17	2:1 acetone & DMAc	0.5	20	10	Viscous solution forms
12	17	2:1 acetone & DMAc	1.5	20	10	Viscous solution forms
13	17	100% acetone	1.5	20	10	Viscous solution forms



Fig. 3.3 Collected CA fibre mat after electrospinning

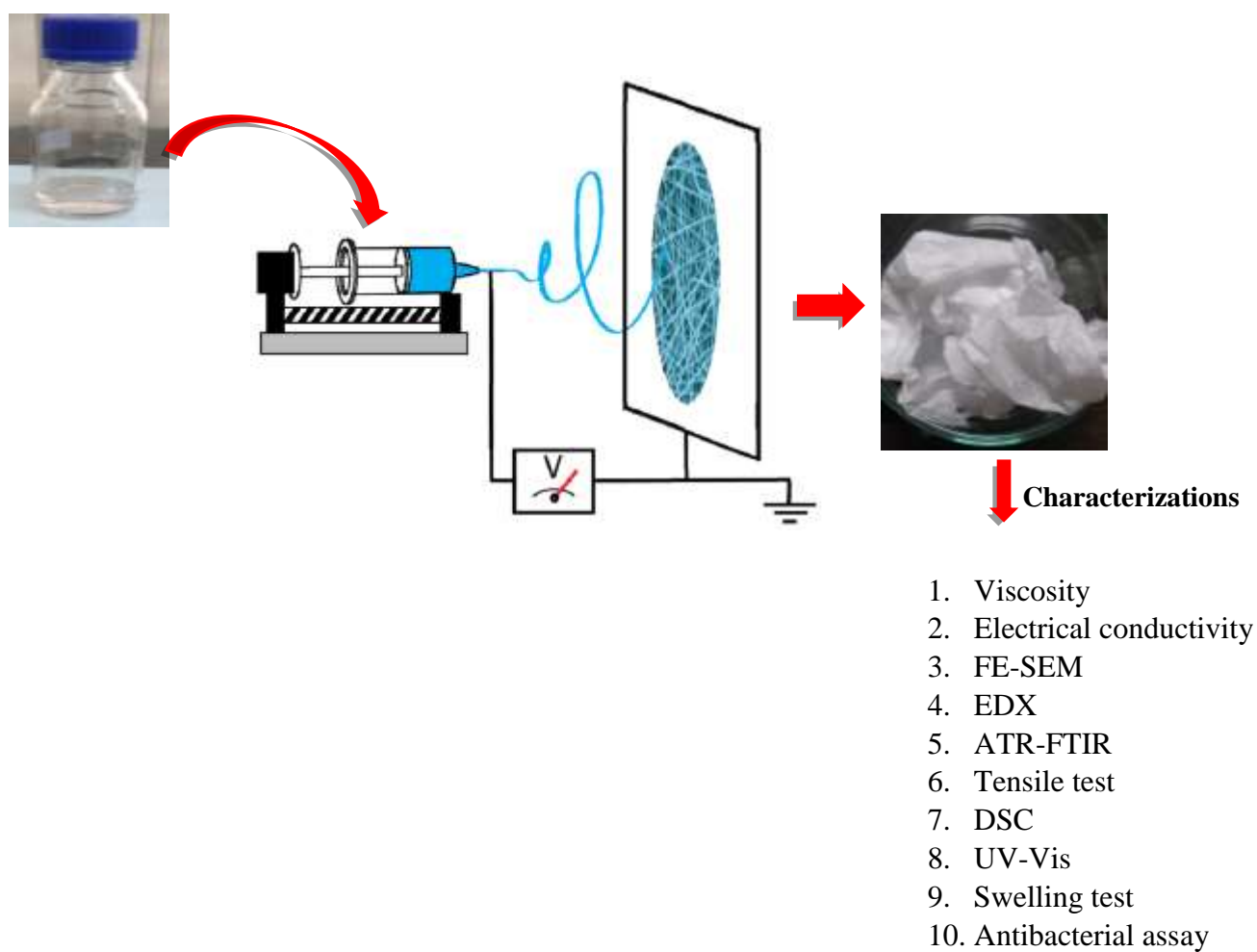


Fig. 3.4 Schematic of electrospinning of CA fibre mat

4. ELECTROSPINNING OF CELLULOSE ACETATE USING DIFFERENT SOLVENT SYSTEMS

4.1 Introduction

Cellulose acetate (CA) is one such polymer which brings with it the advantages of being abundantly available, biocompatible, biodegradable, chemically resistant and low-priced [91-92]. CA fibres fabricated by electrospinning technique comes with the beneficial properties of high porosity, high surface area and roughness. By the virtue of these properties CA electrospun fibres find their widespread applications in wound dressing, filtration, drug release, scaffolds for tissue engineering and biosensors [93].

While electrospinning, it has been observed that different solvent systems can yield uniform fibres without beads, defected fibres with beads, or no fibres at all [94-95]. Moreover, a good solvent for CA does not necessarily ensure its electrospinnability. Previous studies have reported electrospinning of CA with different single and binary solvents such as acetone, chloroform, N,N Dimethylacetamide, N,N Dimethylformamide, acetic acid, methanol, formic acid and blends of them [96-97]. In these studies, variation of molecular weight of polymer and nozzle size has been analyzed on the effect of electrospinning of CA. Other studies extensively discussed the spinning conditions and morphologies of the obtained fibres [98-99]. However, the underlying science correlating the solubility and spinnability of CA and the necessity of binary solvents has not been addressed well so far. Hence, the present work attempted to comprehend the correlation of solubility of CA in different solvents and its electrospinnability for better controlling the electrospinning process using a Teas approach.

Teas approach, has been employed in this study to interpret the solubility behavior of CA in single solvent system of water, acetic acid and pure acetone and binary solvent systems of acetic acid/water and acetone/DMAc. To construct the Teas chart, Hildebrand and Hansen solubility parameters are used. Hildebrand solubility parameter (δ) is the square root of the cohesive energy density (CED) of the material which indicates the relative solvency behavior of a specific solvent [100-101]. Teas chart is a triangular graph which displays three categories of intermolecular forces: dispersion forces (f_d), polar forces (f_p) and hydrogen bonding forces (f_h). This chart can empirically predict the solubility behavior of a polymer in a particular solvent based on

the interaction of these intermolecular forces. Solvents, which are located close on the plot, have similar characteristics while those located far have different solubility properties. The chart also provides an understanding of what happens in the solubility phenomena when solvents are mixed [102]. As a result, solvents, which serve the solubility of CA can be obtained from Teas chart and the spinnability conditions of CA can be superimposed on the chart to prevent trial and error basis for selecting solvents. Recently, Teas chart has been adopted to map the solvents for poly (vinyl alcohol) and polyimide with spinnability conditions effectively superimposed on it [103-104]. Thus, correlation of solubility and spinnability of CA by means of a Teas chart ensures reliable selection of solvents for CA. Furthermore, it would be interesting to study how the electrospinning behavior such as, clogging during electrospinning, viscosity, electrical conductivity and fibre morphology is being affected by polymer concentration and different single and binary solvents.

In this study, the solvents of acetic acid/water, acetone/DMAc and pure acetone were primarily selected as these solvents lie at different locations of the Teas chart. This aided the study of correlating the solubility and spinnability behavior of CA. Furthermore, different concentrations of CA were also used to investigate the effect of concentration on electrospinning behavior and fibre morphology. Analysis of fibre morphology was done to correlate solubility and spinnability of CA. Solution properties and process criteria such as viscosity and electrical conductivity were also studied.

4.2 Experimental

4.2.1 Materials

Cellulose acetate, CA (acetyl content 39.8% and $M_n = 30,000$ by GPC) was acquired from Sigma-Aldrich. The solvents acetic acid (purity 100%), acetone (purity 100%) and N,N-Dimethylacetamide, DMAc (purity 99%) were purchased from Merck.

4.2.2 Electrospinning of CA nanofibres

The electrospinning was carried out by following the procedure mentioned in section 3.2 and 3.4.

4.2.3 Characterization of electrospun CA nanofibres

The morphology of the fibres was studied using FESEM (JEOL JSM 7600F) at an accelerating voltage of 5 kV. Before the observations the samples were platinum coated

using a JEOL JFC-1600 auto fine coater. The viscosity of the CA solutions was measured using a rheometer of Lamy Rheology Instruments (RM 200) with a spindle of value 2 for rotation at room temperature. The electrical conductivities of the solutions were determined with a digital electrometer (HANNA instruments, HI98312). The molecular structure and bonding nature were obtained from ATR-FTIR (Cary 630, Agilent Technologies) spectra. Scanning was carried out from 650 to 4000 cm^{-1} with a resolution of 8 cm^{-1} and a scanning interval of 2 cm^{-1} with 32 repetitious scans averaged per sample.

4.3 Results and Discussion

4.3.1 Solubility and spinnability

A systematic approach has been depicted in this work to study the solvents for CA. The solvents for CA are assessed with the Hildebrand solubility parameter, δ . CA is ideally soluble in solvents or solvent systems with δ in the range of 19.43 – 25.57 $\text{MPa}^{1/2}$. The value of δ for acetic acid, acetone, water and DMAc are 21.4, 19.7, 48.0 and 22.7 $\text{MPa}^{1/2}$, respectively. Hence, all the above mentioned solvents are a good choice for CA except water. The value of δ for mixed solvent system was determined by using the following formula:

$$\delta = \sum \varphi_i \delta_i \quad (5)$$

Here, φ_i represents the volume fraction of the solvent and δ_i is the Hildebrand parameter of that solvent. Using this formula, δ for 3:1 acetic acid/water and 2:1 acetone/DMAc solvent system were found to be 28.05 and 20.70 $\text{MPa}^{1/2}$, respectively.

Moreover, Hansen solubility parameter has also been taken into consideration before solvent selection. The Hansen parameter (δ_t) extended the concept of δ and divided it into three components: dispersion component (δ_d), polar component (δ_p) and hydrogen bonding component (δ_h). This is expressed as follows:

$$\delta_t = \sqrt{(\delta_d^2 + \delta_p^2 + \delta_h^2)} \quad (6)$$

Materials with adjacent values of Hansen parameter (δ_t) are miscible with each other. Thus, Table 1 depicted that the Hansen parameter (δ_t) of water is 47.83 $\text{MPa}^{1/2}$ which lies far from the solubility range of CA. Also, as illustrated by Hansen, an interaction radius (R) of a sphere is formed in a three dimensional coordinate system of dispersion component (δ_d), polar component (δ_p) and hydrogen bonding component (δ_h) [105]. A polymer is potentially soluble in a solvent whose interaction radius (R) is greater than

the distance between the solvent and the centre of the polymer solubility sphere ($D_{(s-p)}$) [102]. As it can be derived from Table 4.1, water again did not meet the criteria to be a solvent for CA as the interaction radius (R) of CA is smaller than the $D_{(s-p)}$ of water. Thus, it was evident that water has no possibility to be a solvent for CA under normal conditions.

Table 4.1. Hansen solubility parameters for CA and solvents [106]

Solvents	Solubility parameter, $\text{MPa}^{1/2}$					
	Hansen Parameter, δ_t	Dispersion Component, δ_d	Polar Component, δ_p	Hydrogen Bonding Component, δ_h	Polymer Solubility Sphere, $D_{(s-p)}$	Interaction Radius, R
Water	47.83	15.60	16.0	42.3	32.47	–
Acetic acid	21.36	14.5	8.0	13.5	2.68	–
Acetone	19.93	15.50	10.40	7.00	5.39	–
DMAc	22.77	16.80	11.50	10.20	5.88	–
2:1 acetone/DM Ac	20.87	15.93	10.77	8.07	–	–
3:1 acetic acid/ H_2O	27.98	14.78	10	20.7	–	–
Cellulose acetate (CA)	19.89	14.90	7.10	11.10	–	12.40

However, CA being soluble in a solvent does not imply to its certain spinnability. Though CA formed homogenous solutions in all the solvents, electrospinning of fibre

was not possible with all the solutions. Hansen method was developed by Teas where he employed a triangular chart, called Teas chart or ternary solubility diagram, with cohesive energy densities to represent solubility limits. In this study, Teas chart also served a role to understand the electrospinnability of CA solution in terms of the fractional parameters [107]. Teas used fractional parameters as:

$$\begin{aligned} f_d &= 100\delta_d/(\delta_d+\delta_p+\delta_h) \\ f_p &= 100\delta_p/(\delta_d+\delta_p+\delta_h) \\ f_h &= 100\delta_h/(\delta_d+\delta_p+\delta_h) \end{aligned} \quad (7)$$

Solubility behavior of polymers in solvents and polymer-solvent interaction can be explicitly studied by using the solubility parameters. Previous studies reported that CA was soluble in both acetic acid and DMAc but none of these solvents alone yielded fibres by electrospinning. Only beaded morphology was obtained [31]. Thus, employing Teas approach as shown in Fig. 4.1, it can be deduced that DMAc and acetic acid can be used as solvents for CA as these lie closer to CA. However, from the experiment it appeared that their solutions cannot be electrospun into fibres. As the solubility parameters of DMAc and acetic acid do not vary largely, it can be concluded that no solvent mixture located on the straight line connecting acetic acid and DMAc are suitable for CA electrospinning. Again, as the value of dispersion force (f_d) approached acetone from DMAc, spinnability improved. Acetone and DMAc have the solvent properties of two extremities which caused the viscosity and surface tension to lie in a moderate range after the mixing of the two. Different ratios of acetone/DMAc had been tried previously from which the ratio of 2:1 acetone/DMAc was proved to be the most versatile as it gives bead free, continuous fibres of CA in the concentration range of 12.5-17 wt% whereas 1:2 acetone/DMAc showed beads [108].

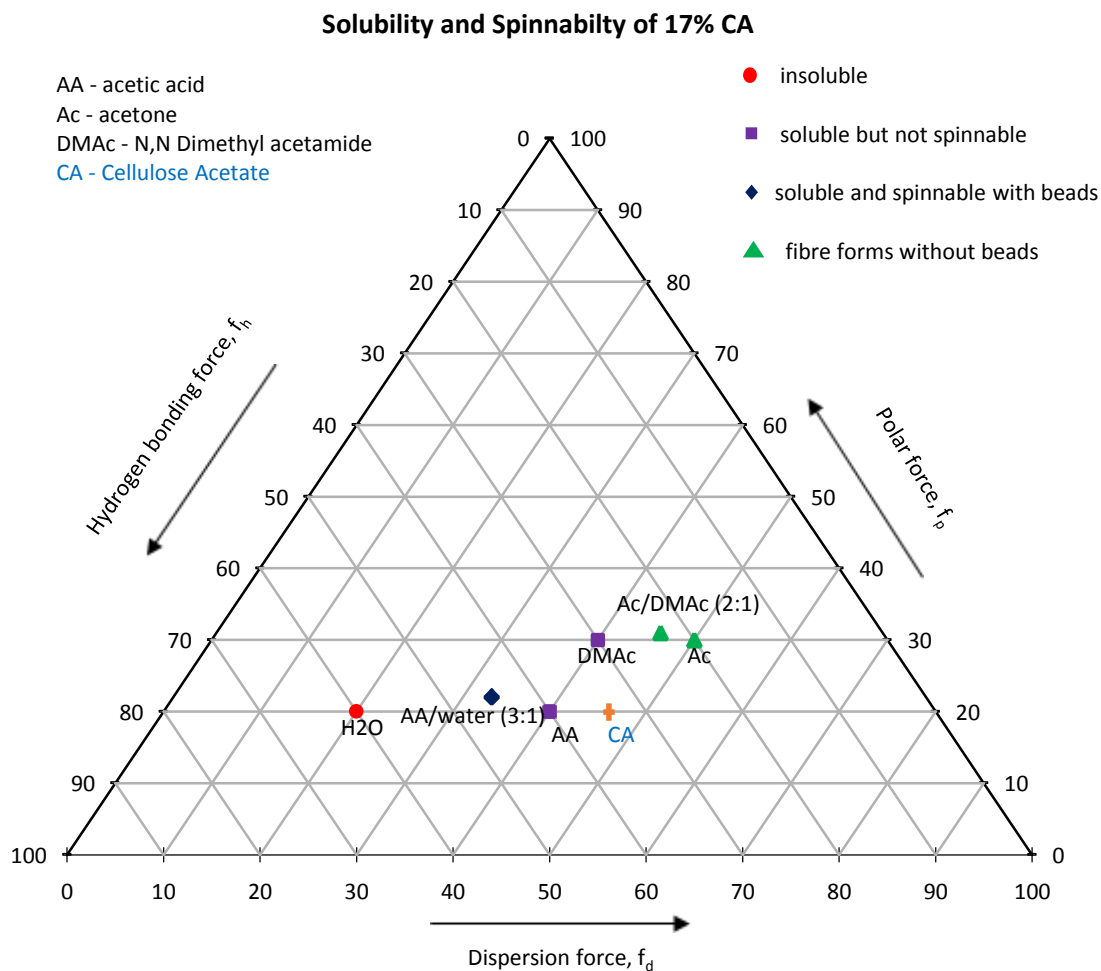


Fig. 4.1 Teas chart to analyze feasibility of solution formation and spinning with different solvents for CA

Moreover, water cannot be used as a solvent for CA and this is evident from the Teas chart as it is located at a greater distance from CA. When 75% acetic acid was added to water, CA dissolved and could be electrospun leading to beaded fibres. It is apparent from the chart that the binary system of acetic acid and water containing less than 75% acetic acid will be inappropriate for electrospinning CA as it will lead to an overall lower dispersion force, f_d . For binary solvents, if the point on the line connecting the two constituent single solvents lie close to that solvent suitable for electrospinning can be regarded as a suitable binary solvent system for the process. Thus, the importance of binary solvent systems becomes evident as two solvents which were previously incompatible for spinning, after blending, developed a solvent system convenient for electrospinning. Hence, the solvents with lower value of dispersion force (f_d) and a

higher value of hydrogen bonding force (f_h) and polar force (f_p) are not suitable for solution forming and spinning of CA. When a mixture of acetic acid/water was explored, fibre formed with beads as water caused dissociation of acetic acid necessary for spinning. In this case, hydrogen bonding force (f_h) did not show any significant effect. It can be interpreted that the interaction of dispersion force (f_d), hydrogen bonding force (f_h) and polar force (f_p) played a vital role in determining the spinnability. Thus, Teas approach can be used as an effective guideline to differentiate between solvents for electrospinning and non-solvents for CA.

4.3.2 Viscoelastic properties of the CA solution

The solution properties of CA dictate the electrospinning behavior. A minimum concentration of polymer is required to cause polymer chain entanglement. Below this minimum concentration, polymer chains overlap but no entanglement takes place which is crucial for electrospinning. It has been seen for CA that increasing concentration favored fibre formation. This change in concentration is associated with the rheological behavior of the solution which controls the morphology of the electrospun fibre. Viscosity is considered to be the key parameter which decides the fibre diameter and whether electrospinning will result in fibre formation. The viscosities measured as showed in Fig. 4.2 of 10, 12, 15, 17 wt% CA in 3:1 acetic acid/water gradually increased with increasing CA concentration. This is due to the increased number of CA molecules and its entanglement in the solution. Increase in viscosity leads to high viscoelasticity which matches with the electrostatic and coulombic repulsive forces associated with the stretching of the electrospinning jet [101]. However, when the viscosity is too high the control of the polymer flow to the tip of the needle is prohibited by the cohesive nature of the solution. The shear stress versus shear rate in Fig. 4.3 also demonstrated the shear thickening effect of CA in both the binary solvent systems.



Fig. 4.2 Viscoelasticity measurement of CA solutions

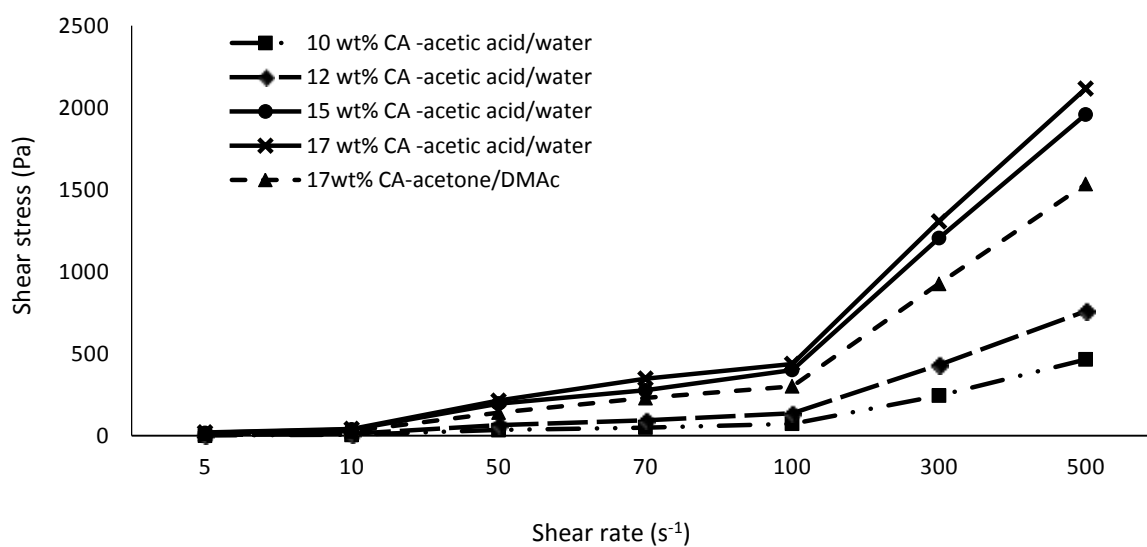


Fig. 4.3 Relationship between shear stress and shear rate of CA solutions with varied concentrations and solvent systems

The formation of a stable jet during electrospinning plays a vital role in the formation of fibres and also depends on the viscoelasticity of the solution. However, this jet is influenced by the process parameters which, if not controlled, can lead to jet splitting and formation of beaded fibres [109]. Beads are considered as defects as they reduce the active surface area of fibres.

Fig. 4.4(a) showed the bending elongated jet which was formed with the 10 and 12 wt% CA solutions. The electrically driven bending instabilities can be explained by Earnshaw theorem of electrostatics which states that a stable structure cannot be created where the elements of structure connect only by Coulomb's law. The Coulomb's interaction energy is minimized by moving the polymer jet in a complicated way by the virtue of its in-built charges [110]. The probable reason for the bending of jet while spinning with 10 and 12 wt% CA can be associated with the increasing repulsive forces between the charges carried by the jet which caused every portion of it to lengthen along a changing direction until the jet solidified [94]. The pendant droplet becomes stable when there is equilibrium between the surface tension of the solution and the electric forces [111-112]. Splitting and blockade at the needle tip occurred in Fig. 4.4(b) when the process was carried out with pure acetone. Due to the high volatility of acetone, it evaporated as soon as it emerged through the needle and clogged the needle tip. This resulted in a tedious task of cleaning the needle tip at regular interval. The stable jet formed in Fig. 4.4(c) when the CA concentration increased and solvent systems included 3:1 acetic acid/water or 2:1 acetone/DMAc. This is the condition when increase in viscosity prevented the partial breakup of the jet and the surface tension was successfully surmounted to form fibres [92].

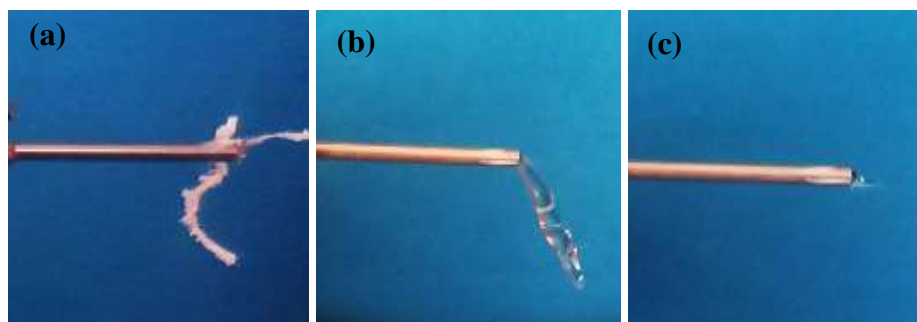


Fig. 4.4 Different needle tip conditions showing (a) clogging of needle tip for CA in pure acetone (b) bending elongation of jet for 10 and 12 wt% CA in 3:1 acetic acid/water and (c) forming of stable cone for 15, 17 and 19 wt% CA in binary solvents

4.3.3 Morphological study of electrospun CA fibre

The morphological observation of Fig. 4.5(a) and 4.5(b) revealed that 10, 12 wt% of CA in 3:1 acetic acid/water did not generate any fibres. Only large beads were observed. This is attributed to the lack of polymer chain entanglement in the solution. As the concentration of CA increased to 15 wt% beaded fibres started forming as showed in Fig. 4.5(c). With the increase in CA concentration, viscosity increased and this drove the polymer chain entanglement to stabilize the jet. Higher viscosity favors the formation of fibres without beads [113-114]. However, the fibre diameters did not alter much on increasing CA concentration in acetic acid/water. Previous study reported that DMAc could not produce fibres but when mixed with acetone fibres were obtained. Due to the presence of acetone, high viscosity and surface tension of DMAc is reduced and formed favorable condition for fibre forming [16].

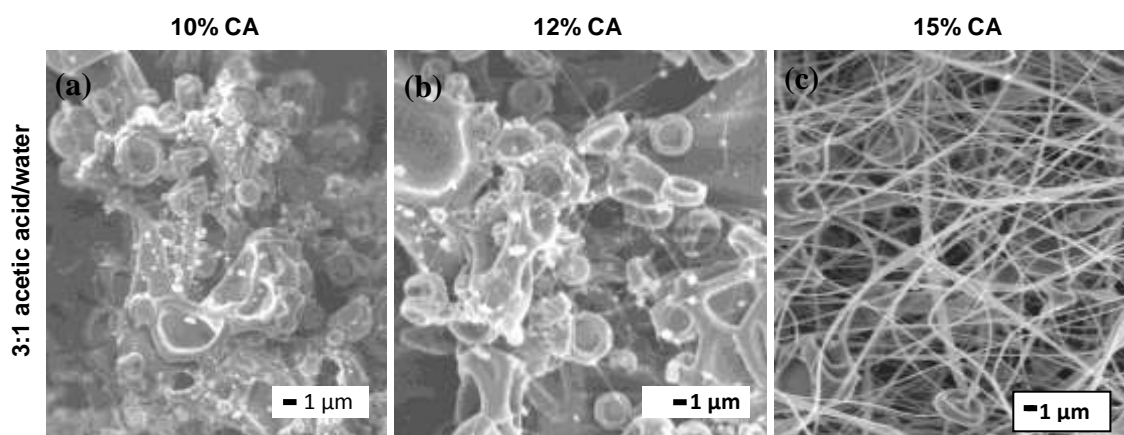


Fig. 4.5 SEM images of (a) 10 (b) 12 and (c) 15 wt% CA in 3:1 acetic acid/water

17 wt% CA in 3:1 acetic acid/water formed fibres with beads, 2:1 acetone/DMAc generated cylindrical bead free fibres and pure acetone constituted of a blend of cylindrical and flat fibres of diameter $\sim 1 \mu\text{m}$ as depicted in Fig. 4.6(a), 4.6(b) and 4.6(c). The 19% CA yielded bead free fibres with 2:1 acetone/DMAc, however, failed to do so with 3:1 acetic acid/water (Fig. 4.6(d) and 4.6(e)). Furthermore, when 19 wt% CA in pure acetone was electrospun a significant change in fibre morphology has been observed. Flat fibres with creased surface and higher transverse sections of 50-60 μm with fused junctions were obtained in this case (Fig. 4.6(f)).

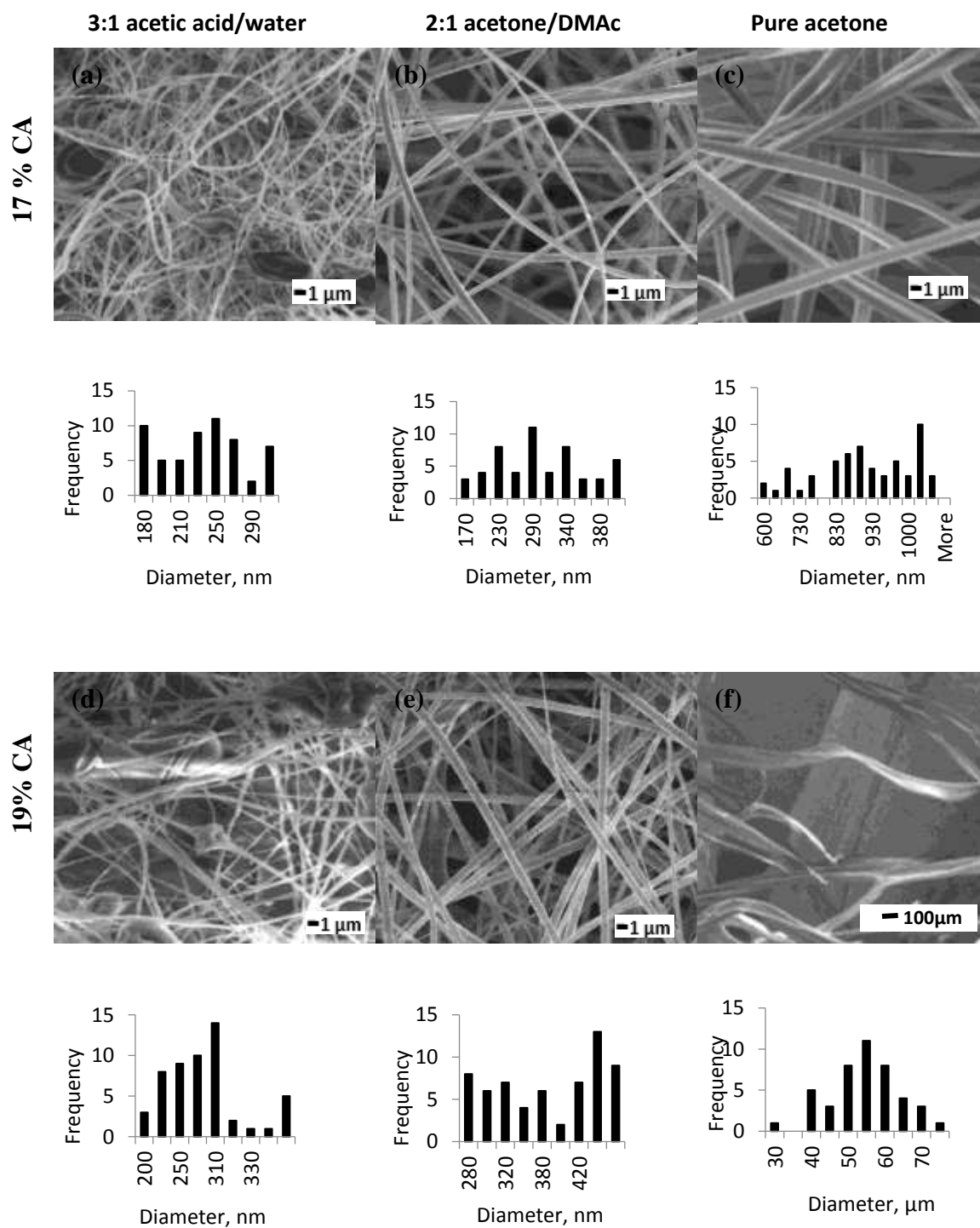


Fig. 4.6 SEM images and fibre size distributions of 17 wt% CA in (a) 3:1 acetic acid/water (b) 2:1 acetone/DMAc and (c) pure acetone ; 19 wt% CA in (d) 3:1 acetic acid/water (e) 2:1 acetone/DMAc and (f) pure acetone.

Ribbon or flat-shaped fibres are due to the fast evaporation of volatile acetone. It has been reported that the tubular fibre skin gets collapsed when a highly volatile solvent is used leading to ribbon like fibres [24].

Therefore, it can be said that different solvent systems lead to different morphology. Table 2 summarized the observed morphology of the electrospun samples of CA with the solvent systems and electrospinning conditions.

4.3.4 Effects of electrical conductivity of solution

A minimum electrical conductivity of the solution is required for electrospinning to take place. An electric field is created between the polymer solution and the collector which causes stretching of the polymer jet towards the grounded collector. Electrical conductivity indicates the available electrical charges on the surface of the polymer solution. The electrical conductivity measured by the conductivity meter as showed in Fig. 4.7 for CA showed a decrease in conductivity with the increase in CA concentration (Fig. 4.8). This was due to the decreased charge density in the solution as the amount of dissociated ions was reduced with increase in concentration due to nonionic nature of CA. The higher concentration of CA also hindered the jet elongation and produced fibres of larger diameter. The mass deposition rate and initial jet diameter during electrospinning decreases with increase in surface charge density and this fact aligned with the explanation of decrease in fibre diameter with increase in electrical conductivity [115].



Fig. 4.7 Electrical conductivity measurement device

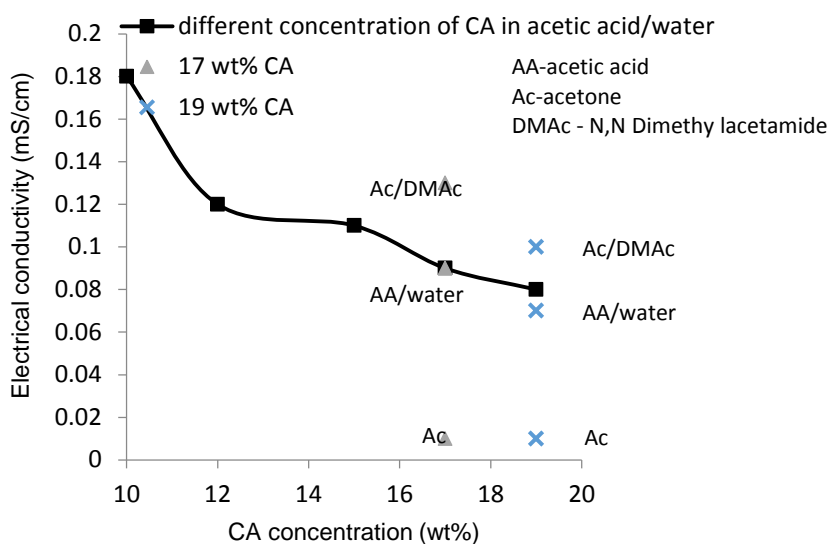


Fig. 4.8 Electrical conductivity of CA for different concentrations and solvent systems

4.3.5 ATR-FTIR

ATR-FTIR spectra of the fibre mats spun with different solvent shows the similar major peaks of CA, which explained there were no chemical changes during formation of solution. CA produced broad absorption bands at 3481 cm^{-1} and 2922 cm^{-1} indicating O-H groups and a sharp peak at 1740 cm^{-1} associated with carbonyl band is the characteristic peak of CA as other peaks may appear in case of cellulose as well. There were also symmetric and antisymmetric bending of methylene groups at 1038 cm^{-1} and 1226 cm^{-1} , respectively in Fig. 4.9 [115-116]. No peaks of solvents were observed due to their evaporation during electrospinning and subsequent heating at 40°C .



Fig. 4.9 ATR-FTIR device

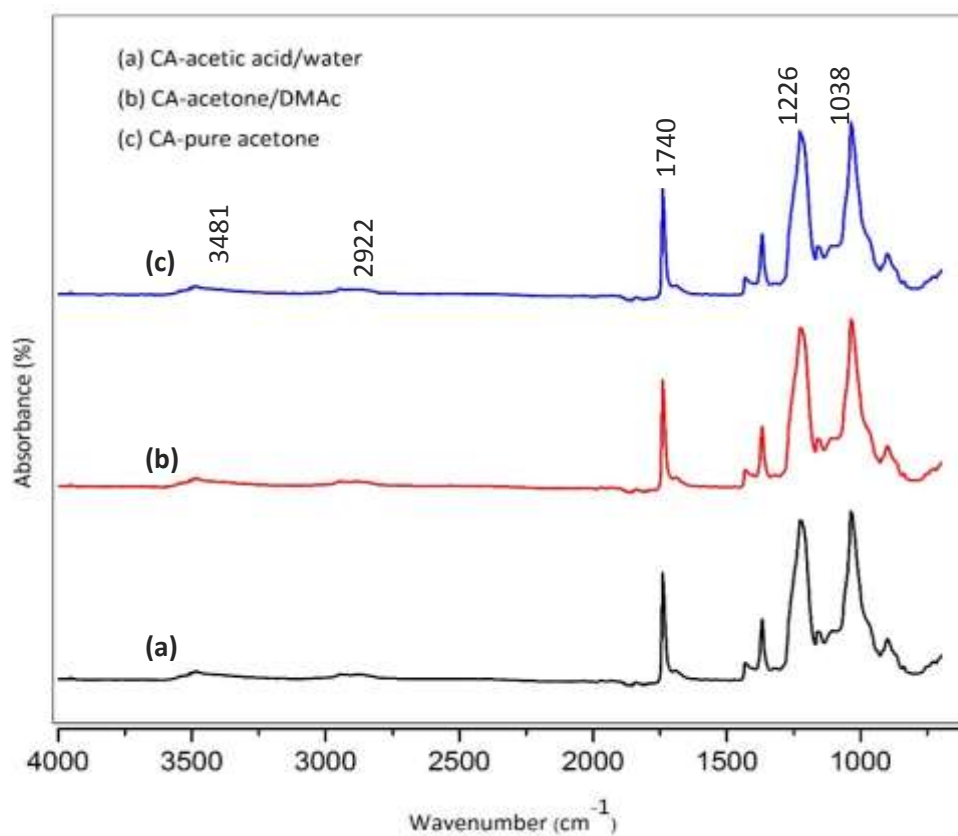


Fig. 4.10 ATR-FTIR spectrum of (a) CA-acetic acid/water (b) CA-acetone/DMAc and (c) CA-pure acetone

5. ELECTROSPINNING AND MODIFICATION OF CELLULOSE ACETATE FIBRE WITH POLYETHYLENE GLYCOL

5.1 Introduction

CA nanofibres obtained by electrospinning possess high surface area-to-mass ratio for efficient mass transportation, optimum flexibility and good interconnectivity of pores which provides fitting conditions for fabricating wound dressing patches [91]. In addition to the aforementioned characteristics, fibre mat for wound dressing also bear some surface roughness to help attachment, proliferation and differentiation of cells. With a view to this, PEG has been electrospun along with CA in this study. PEG is a synthetic, hydrophilic and biocompatible polymer that has been profoundly used in biomedical applications as it does not trigger an immune response. Literature studies revealed that addition of PEG could improve the activity and viability of cells on wound sites [117]. Thus, PEG has been used with CA herein to investigate the surface modification and swelling behavior. In this study, CA fibres were electrospun and its surface was modified with PEG to obtain roughness for better cell proliferation and attain improved swelling properties.

5.2 Materials and Methods

5.2.1 Materials

Cellulose acetate (CA) of molecular weight 30 kDa and silver nitrate (AgNO_3) from Sigma Aldrich were purchased. The used Solvents were acetone and N,N-dimethylacetamide (DMAc). Polyethylene glycol (PEG) of molecular weight 200 and 6000 and citric acid (CT) monohydrate were obtained from Merck. All the chemicals were used without further purification.

5.2.2 Preparation of solutions and electrospinning of nanofibrous mat

Solutions for electrospinning were prepared using 17 wt% CA and 2:1 acetone/DMAc under magnetic stirring for 3 hr at room temperature. The solvent and the quantity of CA has been selected on the basis of our previous study [118]. In order to modify surface properties, the above solution was further stirred with 10, 20, 40 and 80 wt% PEG-200 and 10 wt% PEG-6000 of CA. After obtaining homogenous solution, it was electrospun using an in-house setup. The voltage, feed rate and needle tip to collector distance were 20 kV, 1.5 ml/h and 10 cm respectively. After electrospinning for 2 hr,

the fibre mat was deposited on the Al-foil collector which was then dried overnight at room temperature for further characterizations.

5.2.3 Nanofibres characterization

Chemical and structural analysis were investigated by ATR-FTIR (Cary 630) spectra. Scanning was conducted from 4000 to 650 cm^{-1} with a resolution of 4 cm^{-1} and a scanning interval of 2 cm^{-1} with 64 repetitious scans averaged per sample. Geometric features such as fibre orientation, fibre morphology and fibre diameter were characterized using FESEM (JEOL JSM 7600F) after coating CA fibres with gold at an accelerating voltage of 5 kV. EDX was performed to determine elemental composition of silver loaded fibres. DSC was used to examine the thermal property of the CA samples in a temperature range of 25–400 °C. Approximately 15 mg of the CA samples with PEG 200 and PEG 6000 were analysed in an Al-pan at a heating rate of 10 °C/min.

5.2.4 Swelling measurements

CA, CA-PEG, CA-Ag and CA-PEG-Ag fibre mats were cut into 1 x 1 cm^2 and dried in an oven at 50°C for 4 hr to determine their dry weight (W_d). The dried fibre mats were then soaked in deionized water for 1 hr and 24 hr separately. The swollen fibres were removed from water, dried of excess fluid with filter paper, and weighed to get the wet weight (W_t). The water uptake was calculated from the following formula:

$$\text{Water uptake (\%)} = [(W_t - W_d) / W_d] \times 100 \quad (8)$$

5.3 Results and Discussion

5.3.1 Structural analysis

Molecular structure of CA and structural changes, if any, associated with the addition of PEG to CA are analyzed with ATR-FTIR. The obtained FTIR spectrum of CA and CA-PEG is shown in Fig. 5.1. In the case of pure CA, a broad peak at 3470 cm^{-1} represented stretching of O-H bond, 2881 cm^{-1} displayed the stretching of C-H bond, an intense peak at 1736 cm^{-1} depicted the vibration of the acetate group, C=O. Symmetric and antisymmetric bending of methylene groups were observed at 1239 and 1053 cm^{-1} . The interactions of CA-PEG fibre are confirmed by the FTIR spectra. The hydroxyl group gradually shifted from 3470 cm^{-1} to lower frequency of 3466 cm^{-1} . This shift occurred due to reduction in self-hydrogen bonded O-H groups in CA provided meaningful information about the hydrogen bonding between CA and PEG 200. Carbonyl peak was shifted from 1736 cm^{-1} to 1740 cm^{-1} in CA-PEG fibre which was due to the interactions

of the OH group in PEG and the carbonyl group in CA. Besides, PEG showed its characteristic peak at 1360 cm^{-1} which indicated the crystalline phase of PEG [119-121].

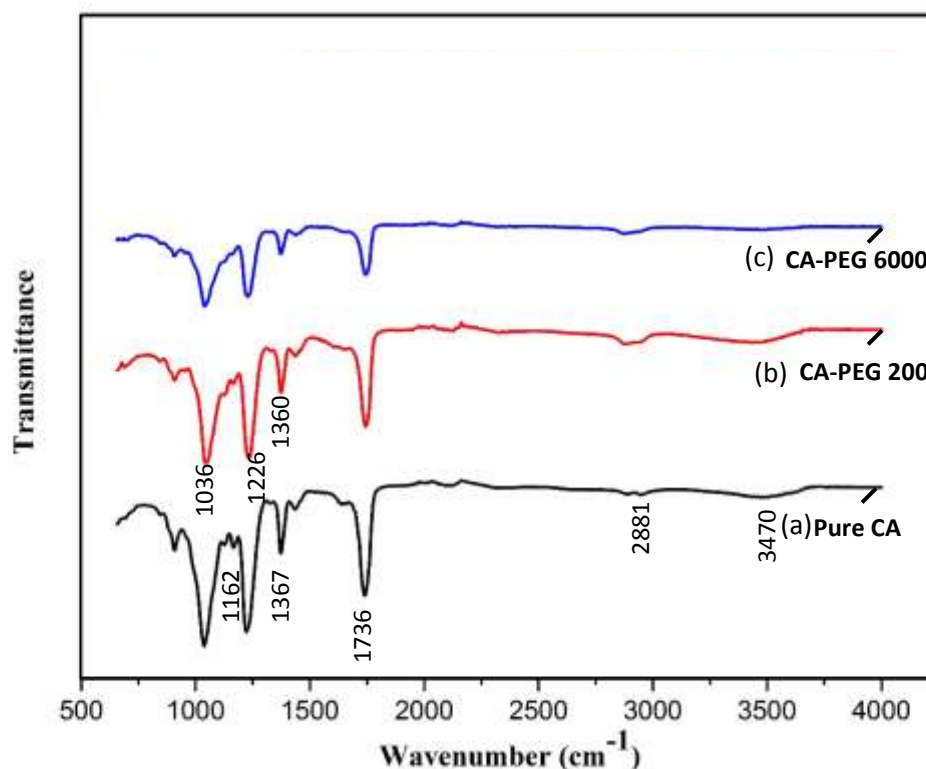


Fig. 5.1 ATR-FTIR spectra of (a) pure CA (b) CA-PEG 200 and (c) CA-PEG 6000

5.3.2 Morphological analysis

FESEM revealed the morphological properties of the electrospun CA and CA-PEG fibre mats in Fig. 5.2. CA in 2:1 acetone/DMAc yielded smooth, uniform fibres with diameters ranging from 250-400 nm as in Fig. 5.2(a). Upon incorporating PEG 200 in different concentrations, a change in fibre morphology was observed. PEG 200 was added in the concentration of 10, 20, 40 and 80 wt% on the basis of the weight of CA into the CA and acetone/DMAc solution. Due to the presence of PEG 200, the smooth surface of the CA fibres appeared striated and rough as showed in Fig. 5.2(b-e). These striations were maximised for 20 and 40 wt% PEG in CA. The diffusivity rate of PEG was much slower than acetone/DMAc and thus PEG in the solvent took more time to accumulate on the surface forming striated layers [122]. However, 80 wt% PEG did not

result in much of the striated fibres except for some wavy surfaces indicated in Fig. 5.2(f).

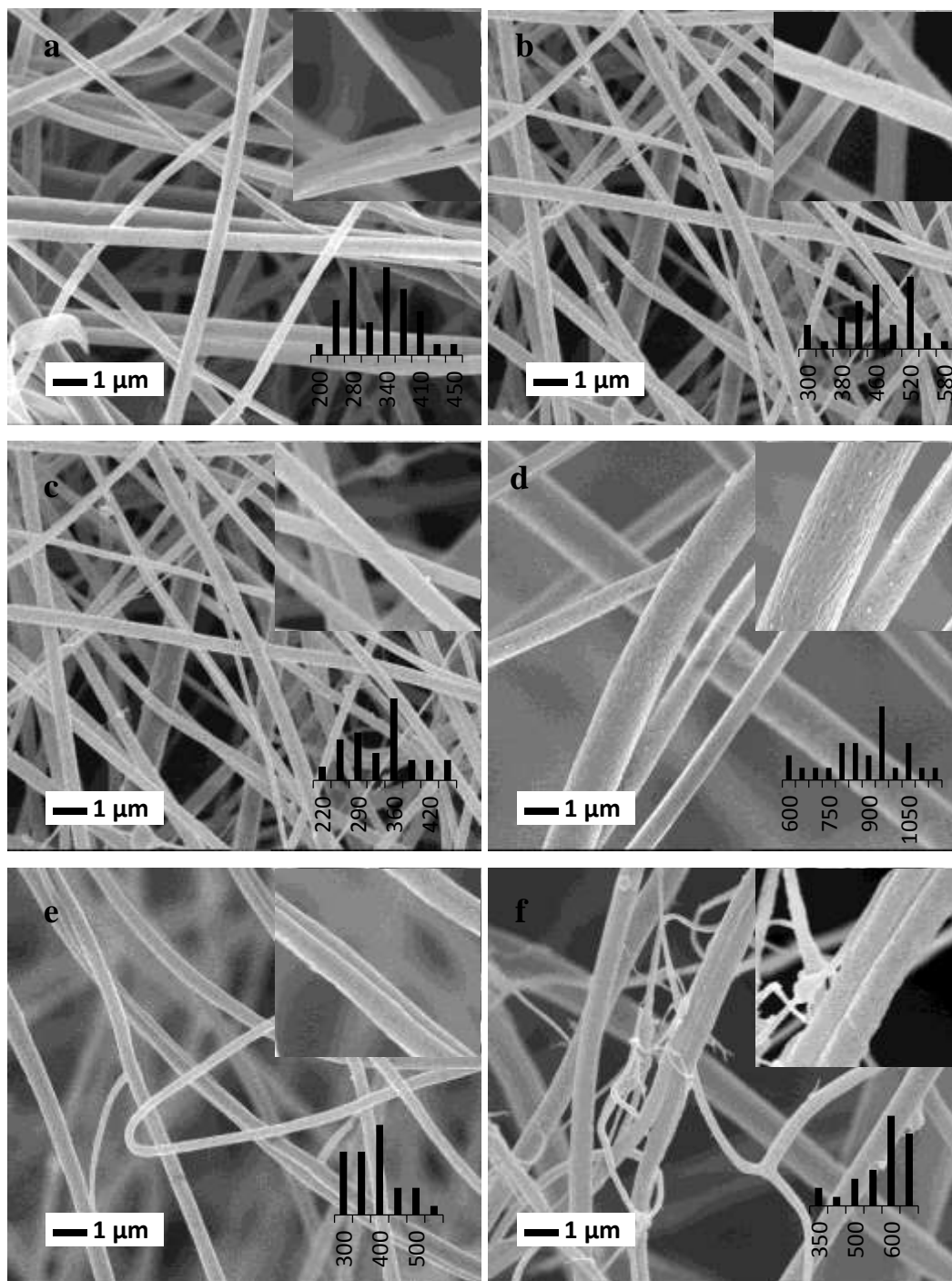


Fig. 5.2 FESEM (10000X) of fibres electrospun in a) CA-solvent b) CA-solvent-10wt% PEG 200 c) CA-solvent-20wt% PEG 200 d) CA-solvent-40wt% PEG 200 e) CA-solvent-80wt% PEG 200 and f) CA-solvent-10wt% PEG 6000. Inset shows the magnified images (30000X) along with fibre diameter distribution.

CA solution electrospun with 10 wt% PEG 6000 also showed rough fibre surface. However, electrospinning with high molecular weight PEG was inconvenient as meagre amount of fibre mat got deposited. Due to higher molecular weight of PEG, the CA solution turned quite viscous which suppressed the elasticity and hindered the flow of solution. Also, it suppressed the formation of striated fibres as PEG 6000 resulted in greater polymer chain entanglement with CA which produced more dense structure [123].

Previous literature presented that addition of PEG into CA did not yield grooves or striations until the fibres were being washed [124-125]. In this study, striated morphology was obtained without any washing of the fibre. This topographical modification of electrospun CA fibre to obtain a rough surface texture has an advantage for cell adhesion. The surface roughness of the fibre mats allowed more air to be trapped between the interfaces than that of smooth fibres. This facilitated the permeation of oxygen and nutrients between the wound and the external surrounding [126].

5.3.3 Thermal analysis

DSC thermograms in Fig. 5.3 were recorded to investigate the thermal behaviour of CA-PEG 200 fibre mats. CA displayed an endothermic event located at around 50-110° C which is attributed to the outflow of water (desorption of water). Desorption occurs due to presence of residual moisture or low boiling point solvents and varies on the account of degree of substitution in CA [127]. The glass transition temperature, T_g , of CA is located over a range of 135-200°C for CA when the base gradually shifted upwards. An endothermic peak at 220-230°C corresponded to the melting range of CA [31]. On the addition of PEG 200, the T_g shifted to a lower temperature range of 70-110°C whereas, no melting peak was observed within a temperature region of 250°C. This degraded shift in T_g can be interpreted as such that low molecular PEG, acting as a plasticizer, interrupted the physical interactions of CA chains and increased the chain mobility and finally, resulted in lower T_g [121].

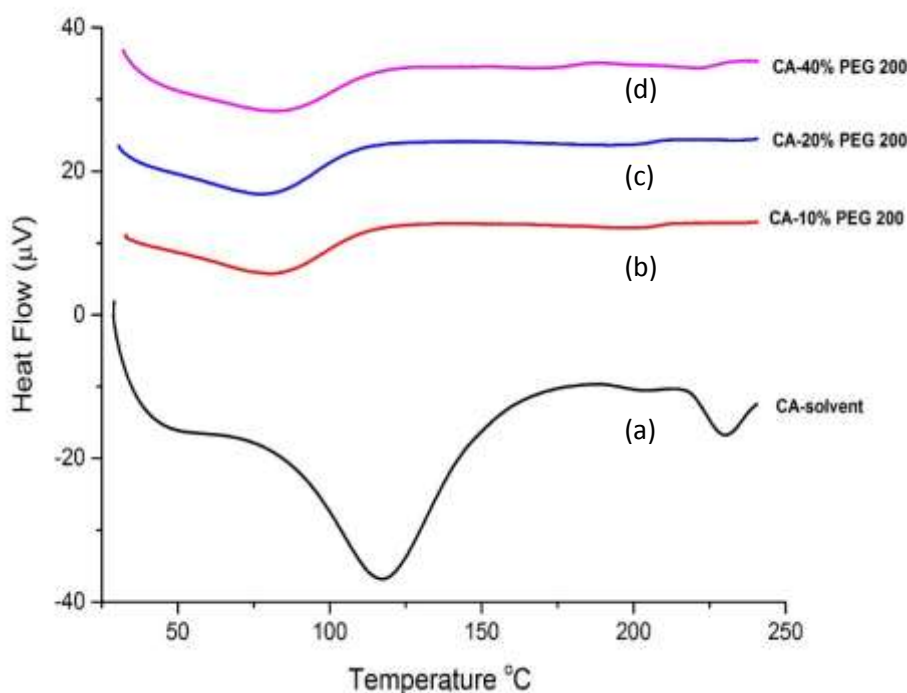


Fig. 5.3 DSC thermogram of (a) CA-solvent (b) CA-10%PEG 200 (c) CA-20%PEG 200 (d) CA-40%PEG 200 fibre

5.3.4 Swelling behaviour analysis

The capacity of the fibre mat to retain body fluid, metabolites and wound exudates is another essential feature of wound dressing patches [127]. Fig. 5.4 represented the swelling characteristics of CA fibre mats with and without PEG 200 in deionized water. Deionized water has been used here because it matches with the pH of wound exudates that is alkaline in nature. Moreover, wound exudates mainly consist of watery substances that need to be absorbed by the dressing for rapid healing. As seen from the bar chart, the water content of CA fibre mat was comparatively low and was around 350% after 24 hr immersion. With the presence of PEG 200, the ability to retain water increased to 680%. This phenomenon was attributed to the hydrophilic nature of PEG. Coming in contact with water, PEG dissolved away leaving porous network in the fibre mat which retained more water. Also, the rough surfaced fibre that was created on adding PEG built bridges along the surfaces and improved water holding capacity than that of CA fibre alone [128].

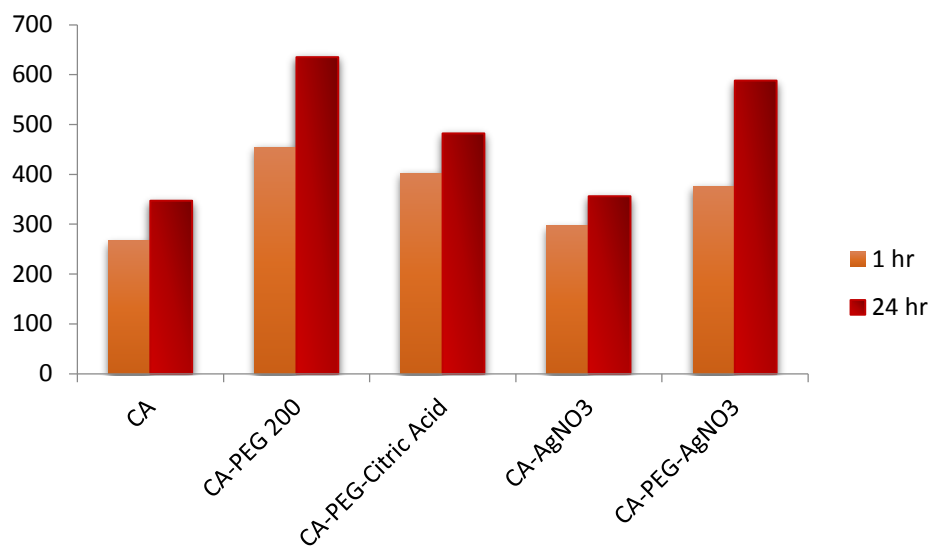


Fig. 5.4 Water uptake of different fibre mats at 1 and 24 hr

6. FUNCTIONALIZATION OF CA FIBRE WITH AgNO₃ AND ASSESSMENT OF ANTIBACTERIAL ACTIVITY

6.1 Introduction

In order to integrate antibacterial properties into the CA-PEG 200 based fibres, AgNO₃, as antimicrobial agent, has been introduced into the fibres. Silver has emerged as a reasonable choice for preventing or treating infections caused by chronic wounds. Ag nanoparticles embedded in polymer matrix can continuously discharge long-lasting and powerful antibacterial effect. Ag nanoparticles have been produced using different methods: electrochemical method [129-132], thermal decomposition, laser ablation, microwave irradiation and sonochemical synthesis [133]. However, the chemical way is often employed to obtain Ag particles [134]. Electrospinning of polymer solution with silver particles to form silver grafted fibre mat has been reported earlier where a reducing agent such as N,N dimethylformamide (DMF) or sodium borohydride (NaBH₄) and a stabilizing or capping agent such as polyvinyl pyrrolidone (PVP) were added to the polymer solution for reducing AgNO₃ into finely dispersed Ag particles [135-137]. Also, UV-irradiating, and dipping of electrospun fibres into previously reduced AgNO₃ solution are widespread methods for getting Ag nanoparticles [138-139].

Ag nanoparticles were successfully grafted into the fibre surface which showed strong antibacterial activity against *E.coli* and *S. aureus*. Ag is non-toxic to human cell, but toxic to bacteria due to its affinity for protein and nucleic acid. This study differed from earlier works in the way that AgNO₃ was reduced in-situ via the solvents used for electrospinning CA i.e. acetone/DMAc. To the best of our knowledge, no works have reported synthesis of Ag nanoparticles using acetone/DMAc solvent system. Finely dispersed Ag nanoparticles were observed without any agglomeration. The structure

morphology, mechanical stability, and water-uptake and surface properties of the produced material were studied. Antimicrobial activity were conducted to highlight the potential use of these electrospun mats for wound healing.

6.2 Materials and Methods

6.2.1 Materials

Cellulose acetate (CA) of molecular weight 30 kDa and AgNO₃ from Sigma Aldrich were purchased. The used Solvents were acetone and N,N-dimethylacetamide (DMAc). Polyethylene glycol (PEG) of molecular weight 200 and 6000 and citric acid (CT) monohydrate were obtained from Merck. All the chemicals were used without further purification.

6.2.2 Preparation of solutions and electrospinning of nanofibrous mat with AgNO₃

The solutions with CA and AgNO₃ were prepared according to the procedures described in section 3.3 and electrospun following the procedure in section 3.4.

6.2.3 CA-PEG-Ag nanofibres characterization

Chemical and structural analysis were investigated by ATR-FTIR (Cary 630) spectra. Scanning was conducted from 4000 to 650 cm⁻¹ with a resolution of 4 cm⁻¹ and a scanning interval of 2 cm⁻¹ with 64 repetitious scans averaged per sample. Geometric features such as fibre orientation, fibre morphology and fibre diameter were characterized using FESEM (JEOL JSM 7600F) after coating CA fibres with gold at an accelerating voltage of 5 kV. EDX was performed to determine elemental composition of silver loaded fibres. The tensile tests were performed on electrospun fibre mats with Shenzhen Wance Testing machine using a load cell 10 N. The samples were of 5mm x 30mm x d, where d is the thickness of the sample. A preload of 0.001 N was applied and a strain rate of 2 mm/min and a gauge length of 20 mm were used. DSC was used to examine the thermal property of the CA samples in a temperature range of 25–400 °C. Approximately 15 mg of the CA samples with PEG 200, PEG 6000, citric acid and AgNO₃ were analysed in an Al-pan at a heating rate of 10 °C/min. UV–visible spectra were recorded on a UV-3100 Spectrophotometer.

6.2.4 Antibacterial evaluation

Antimicrobial activity assessment of the fibres was carried out using Colony Forming Unit (CFU) method against *E. coli* and *S. aureus*. Agar and nutrient broth solutions were prepared as in Fig. 6.1(a) and (b). Both types of cultured bacteria were grown in a test tube containing 1 part nutrient broth and 9 part saline. After 1 day, this broth solution was diluted to 1×10^5 CFU/ml.

Now, the Ag-loaded fibre mat was cut into a square size and sterilized under UV light in a bio-cabinet for 20 min. The sterilized samples were placed in the diluted broth-saline solution and vigorously shaken to elute bacteria. Also, this sample filled test tubes were incubated overnight at 37°C . Next, $100\mu\text{l}$ of the sample loaded broth-saline solution is spread on agar plates and incubated for colony counting. The antibacterial effectiveness (AE) was calculated as the reduction of CFU on the test sample in comparison with control sample:

$$AE = [(A-B)/A] \times 100\% \quad (9)$$

Where, A and B are the number of viable bacterial colony forming units (CFUs) recovered from the blank control and treated sample specimen after 24 h, respectively.

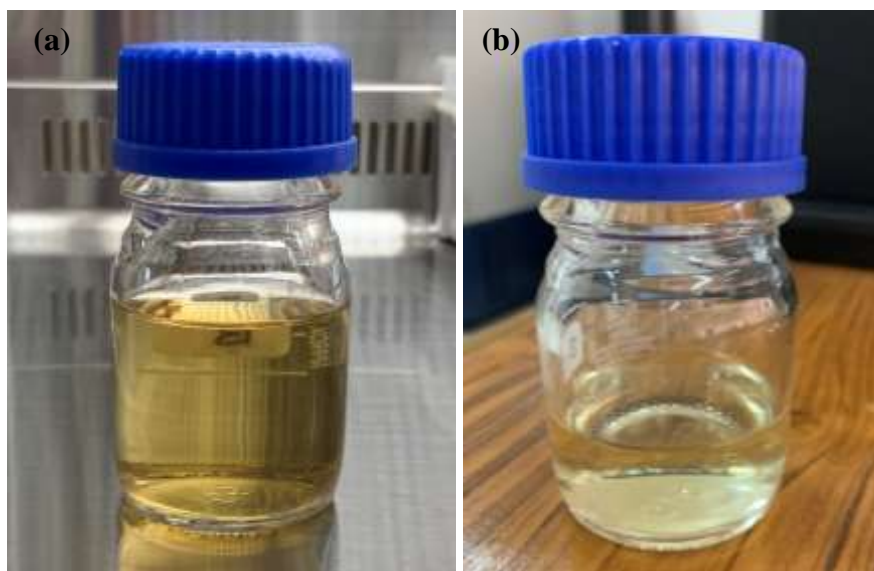


Fig. 6.1 (a) Agar solution (b) Nutrient broth solution

6.3 Results and Discussion

6.3.1 Structural analysis

Molecular structure of CA and structural changes, if any, associated with the addition of PEG and AgNO₃ to CA are analyzed with ATR-FTIR. The obtained FTIR spectrum of CA, CA-PEG and CA-PEG-Ag is shown in Fig. 6.2. In the case of pure CA, a broad peak at 3470 cm⁻¹ represented stretching of O-H bond, 2881 cm⁻¹ displayed the stretching of C-H bond, an intense peak at 1736 cm⁻¹ depicted the vibration of the acetate group, C=O. Symmetric and antisymmetric bending of methylene groups were observed at 1239 and 1053 cm⁻¹. The shifting of C-O bond from 1238 cm⁻¹ to slightly lower frequency of 1238 cm⁻¹ was attributed to the binding of C=O and C-O with silver particles [115-116].

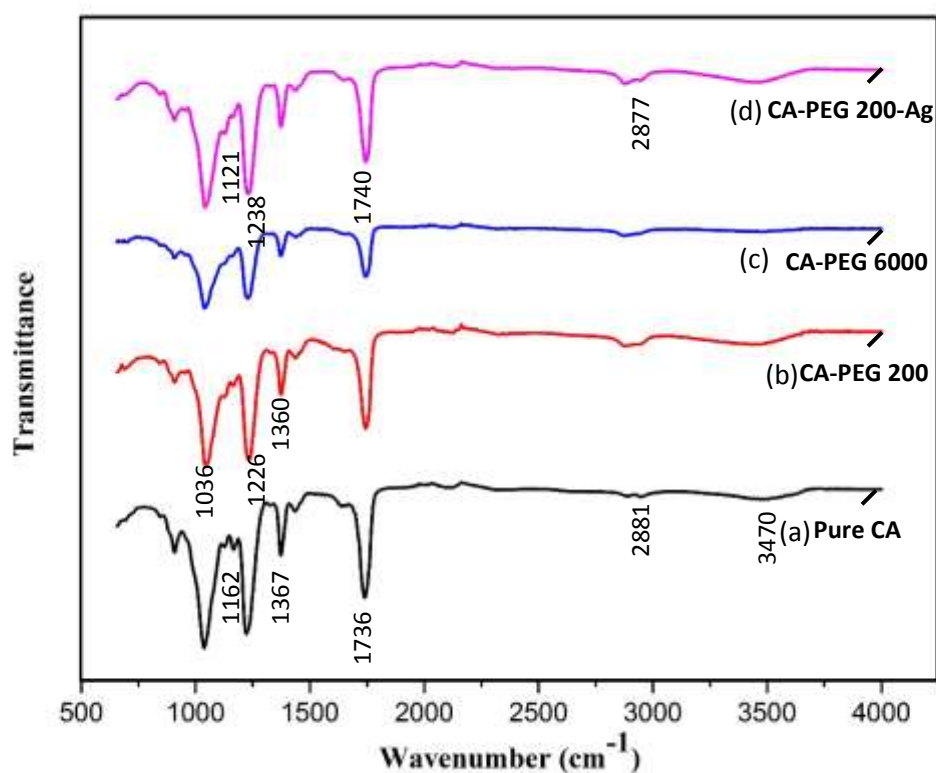


Fig. 6.2 ATR-FTIR spectra of (a) Pure CA, (b) CA-PEG 200 (c) CA-PEG 6000 and (d) CA-PEG 200-Ag fibre

6.3.2 Morphological analysis

Beadless and homogenous fibres were obtained from CA and PEG 200 in 2:1 acetone/DMAc solvent. Due to the presence of PEG 200 striated morphology was observed. This was due to the low molecular weight of PEG 200 which interrupted the CA chain and imparted flexibility to it. Silver nitrate was reduced to silver nanoparticles and adhered to the fibre surface as showed in Fig. 6.3. The particle size was determined to be ~10 nm. Fibres are of uniform size of diameter ~200 nm. EDX analysis in Fig. 6.3(c) represented the elemental composition of the fibre and confirmed the presence of silver at 3.00 keV which is the typical absorption peak of Ag nanocrystallites [140].

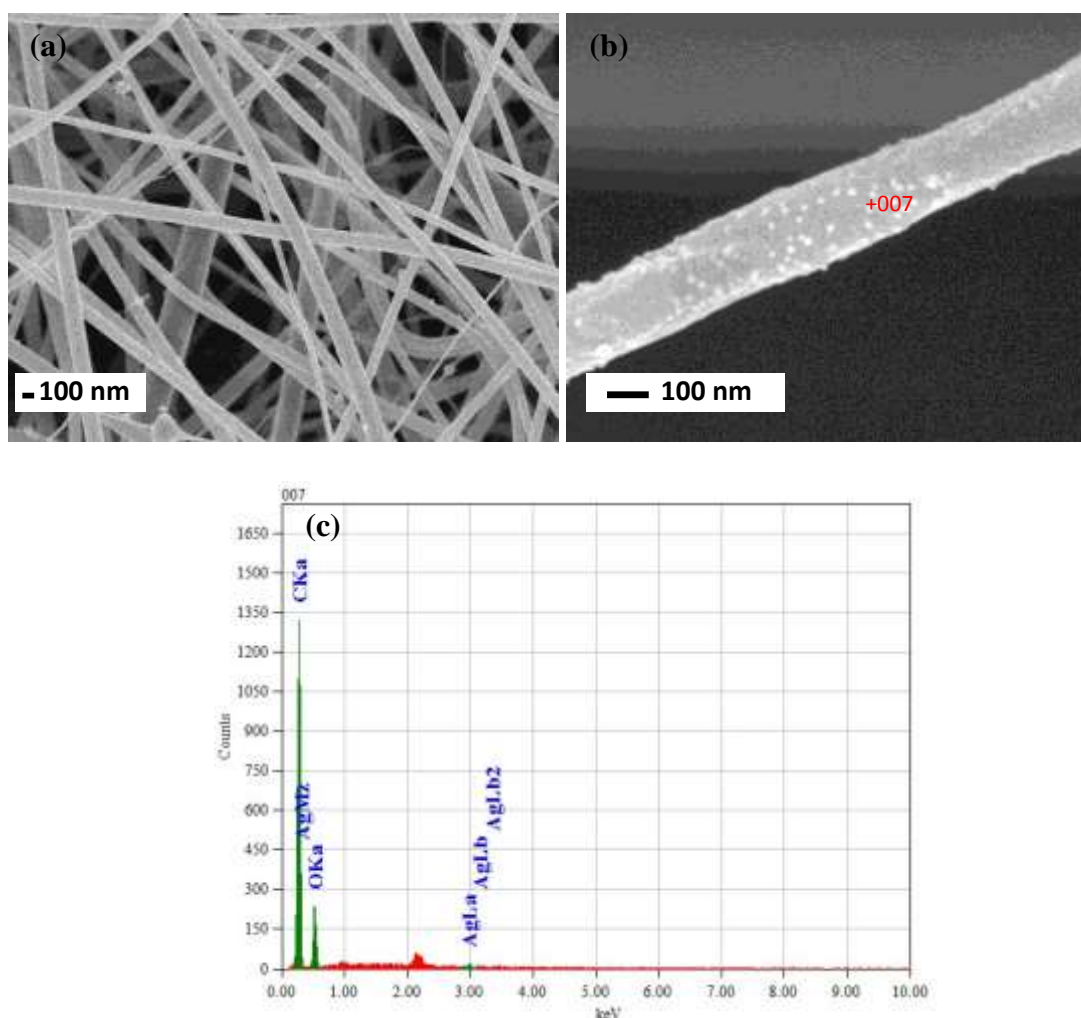


Fig. 6.3 FESEM of CA-PEG 200-Ag fibre (a) 10000X (b) 100000X and (c) EDX of CA-PEG 200-Ag fibre

6.3.3 UV-Vis analysis

The UV-Visible spectrophotometer and UV-Visible spectrum of CA-PEG 200 with 1 wt% AgNO₃ fibre has been shown in Fig. 6.4 and Fig. 6.5 respectively. The maximum absorbance at 420 nm in the spectrum was associated with the plasmon peak which corresponded to the surface-bound Ag nanoparticles [136]. Solution of Ag nanoparticles showed distinctive color arising from their tiny dimensions. The spectral position of plasmon band absorption as well as its width was determined by the size and shape of the Ag nanoparticles. From the Fig. 6.5 it can be deduced that a relatively narrower peak was obtained which corresponded to smaller size of the particles [137].



Fig. 6.4 UV-Vis spectrophotometer

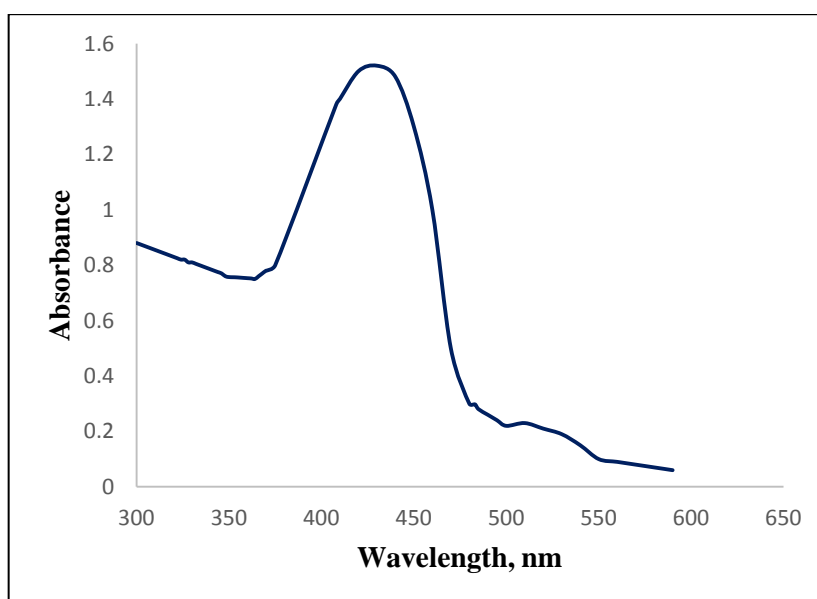


Fig. 6.5 UV-Vis spectrum of CA-PEG 200 nanofibre containing 1 wt% AgNO₃

6.3.4 Mechanical property analysis

The tensile strength and elongation were determined to estimate the mechanical properties of unmodified CA fibre mat and modified mat with CT and Ag nanoparticles. Fig. 6.6 depicted the failure of the fibre during tensile loading and the corresponding stress-strain curves of the samples were shown in Fig. 6.7. The tensile strength obtained for unmodified CA fibre was significantly lower with a value of 0.002 MPa. However, when modified with 10 wt% CT, the stress value increased to 0.033 MPa. This increase in strength had been achieved without any heat treatment. On the other hand, with the grafting of Ag nanoparticles in CA fibre, it could sustain higher load and the ultimate tensile strength and elongation at break increased moderately. This is imputed to the fact that Ag nanoparticles could bear the increased load in the fibre surface [110]. However, the modulus was the maximum for CA-PEG 200-Ag fiber mat in Fig. 6.7(b). Moreover, the tensile strength values obtained in this study did not comply with previous literatures. This could be due to the impurities and fibre alignment which had immense effect on the mechanical tests.



Fig. 6.6 Failure of the CA fibre mat during tensile test

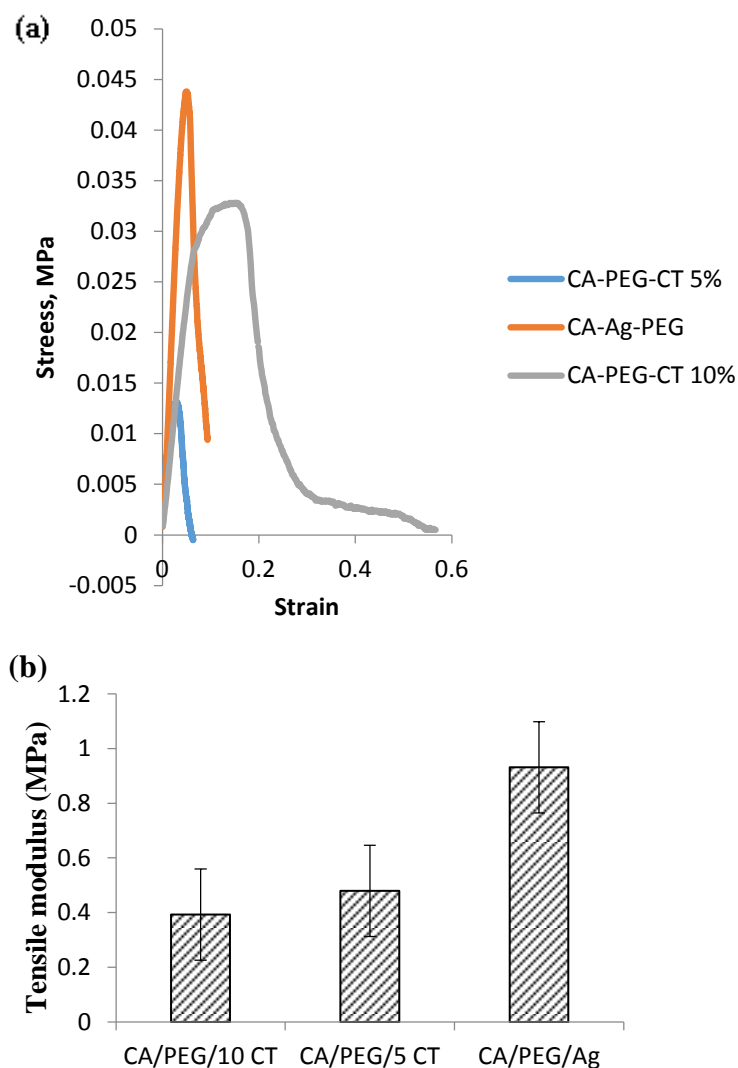


Fig. 6.7 (a) Stress vs strain plot for CA fibres (b) Tensile modulus diagram for CA, CA-PEG 200 and CA-PEG-Ag fibres

6.3.5 Thermal property analysis

A broad endothermic peak between 25-100°C was observed for CA-PEG-Ag fibre sample for desorption of water in the Fig. 6.8. Also, a sharp rise in base for this sample was also evident and corresponded to a T_g of ~130°C. Thus, addition of silver nanoparticles affected the thermal behaviour of CA fibre. The value of T_g which dropped down due to addition of PEG increased on incorporating Ag particles on the fibre. Also, the melting peak of CA fibre alone has been shifted to higher temperature on adding PEG and Ag. This additions improved the thermal stability of the electrospun CA fibre.

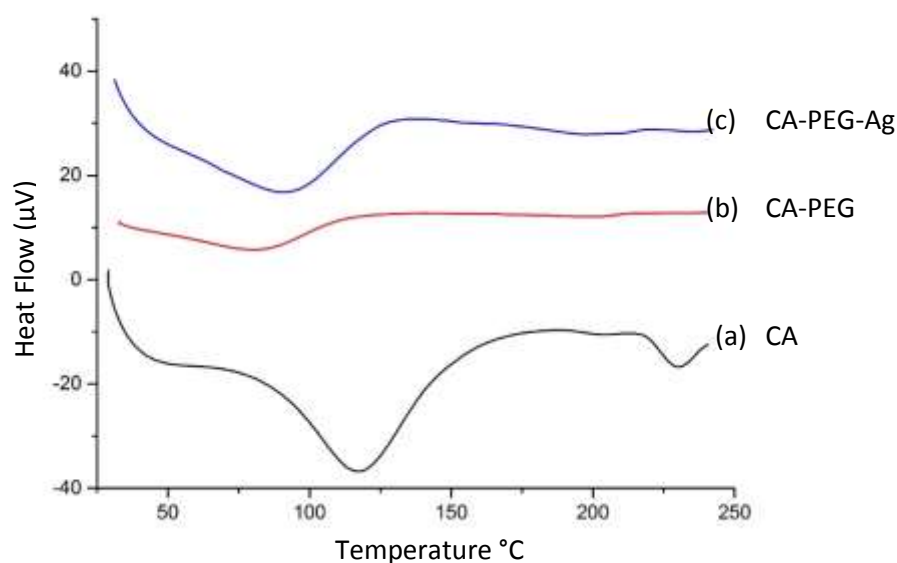


Fig. 6.8 DSC thermogram of (a) CA, (b) CA-PEG 200 and (c) CA-PEG-Ag fibre

6.3.6 Antibacterial assay

Bacteria generated in the wound site can consume up the nutrients required for cell repair. Therefore, functionalization of wound healing materials with antibacterial agents is necessary. The antibacterial capacity of Ag-loaded CA-PEG 200 fibre mat was explored through viable colony counting method and represented in Fig. 6.9. When the bacterial inoculum was treated with CA-PEG 200 fibre, it did not exhibit any bacterial killing. Thus, CA-PEG 200 fibre mat do not have antibacterial properties in it. The antibacterial efficacies of Ag nanoparticles loaded CA-PEG 200 fibre mat when tested against *E. coli* was found to be 97.5% and 100% for *S. aureus*. This indicated that electrospun CA fibre mat with Ag nanoparticles exhibited robust antibacterial activity against gram negative *E. coli* and gram positive *S. aureus*. Relatively, antibacterial effect against *E. coli* was somewhat lower than that against *S. aureus*. This can be attributed to the different nature of cell wall between Gram-positive and Gram-negative bacteria. The cell wall of *E. coli* consists of lipids, proteins and lipopolysaccharides (LPS) which provides effective protection against biocides whereas, the cell wall of Gram-positive bacteria, such as *S. aureus* does not consist of LPS.

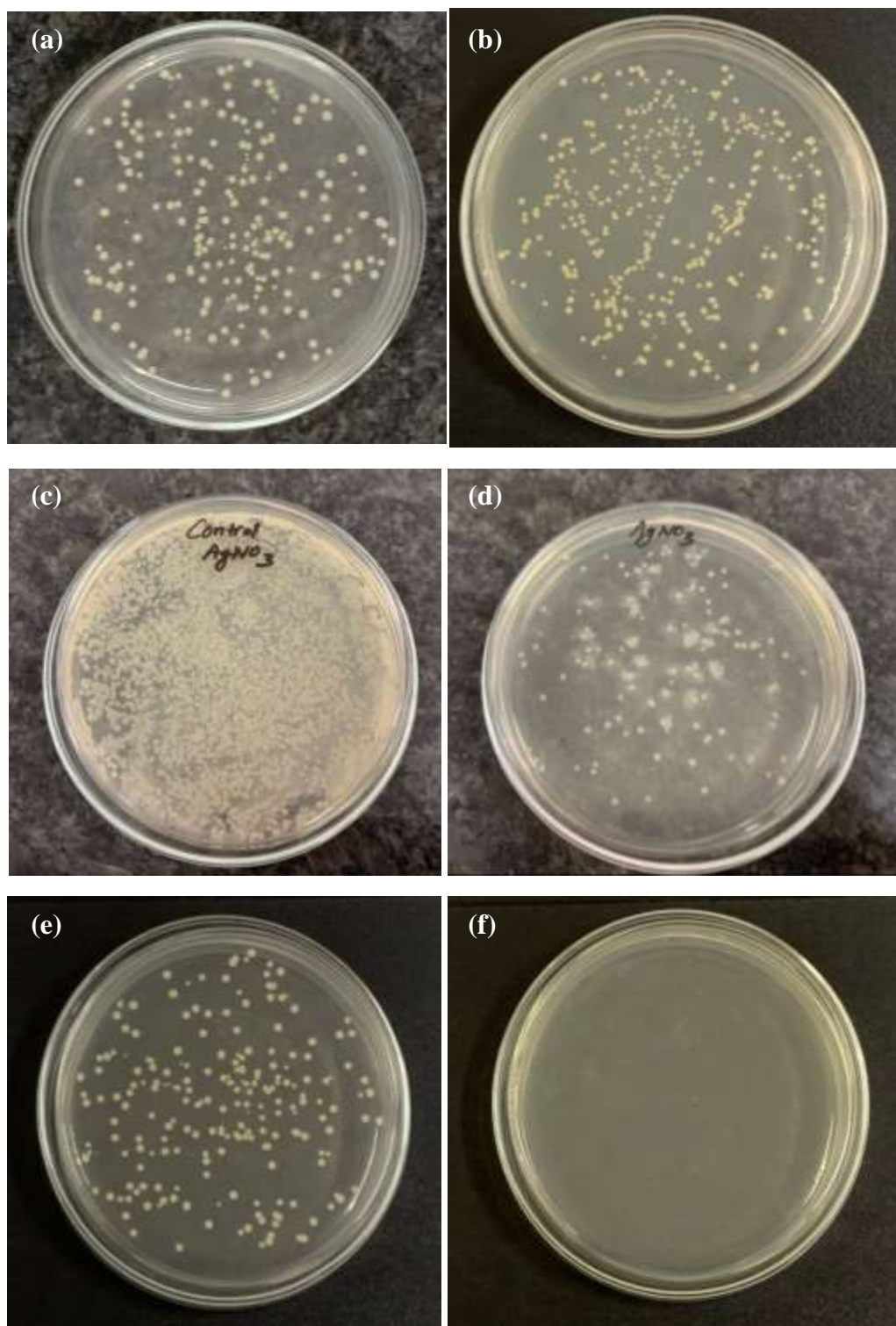


Fig. 6.9 Antibacterial test results for (a) *E. coli* blank control (b) *E. coli* incubated with CA-PEG 200 fibre (c) *E. coli* blank control (d) *E. coli* incubated with Ag loaded CA-PEG 200 fibre (e) *S. aureus* blank control (f) *S. aureus* incubated with Ag loaded CA-PEG 200 fibre

7. SUMMARY OF THE RESULTS

This research work of electrospinning and functionalizing CA divided the whole experiment into three stages. A summary of the findings and their comparisons have been made here for better analysis of the results obtained.

Table 7.1 Comparisons of electrical conductivity

Samples	Electrical Conductivity
10 wt% CA+75% acetic acid	0.18
12 wt% CA+75% acetic acid	0.12
15 wt% CA+75% acetic acid	0.52
17 wt% CA+75% acetic acid	0.09
19 wt% CA+75% acetic acid	0.08
17 wt% CA+2:1 acetone/DMAc	0.13
17 wt% CA+acetone	0.01
19 wt% CA+2:1 acetone/DMAc	0.11
19 wt% CA+acetone	0.02

CA in acetic acid/water showed a decrease in conductivity with the increase in CA concentration. However, higher conductivity was observed for CA in acetone/DMAc at a fixed concentration.

Table 7.2 Comparisons of morphological structures

Solvent Systems	Observations				
	10 wt% CA	12 wt% CA	15 wt% CA	17 wt% CA	19 wt% cA
3:1 acetic acid/water	Only beads were formed	Only beads were formed	Uniform fibres with beads were formed.	Uniform fibres with beads were formed. Fibre diameters were around 200-350 nm	Uniform fibres with beads were formed.
2:1 acetone/DMAc	-	-	-	Uniform, bead less nanofibers were formed with diameter 200-300 nm	Uniform, bead less nanofibers were formed with diameter 200-400 nm

Solvent Systems	Observations				
	10 wt% CA	12 wt% CA	15 wt% CA	17 wt% CA	19 wt% cA
Pure acetone	-	-	-	It constituted of a blend of cylindrical and flat fibres of diameter ~1 μm .	19 wt% CA in pure acetone produced flat fibres with creased surface and higher transverse sections of 50-60 μm were obtained
2:1 acetone/DMAc	10 wt% PEG 200 + 17 wt% CA	20 wt% PEG 200 + 17 wt% CA	40 wt% PEG 200 + 17 wt% CA	80 wt% PEG 200 + 17 wt% CA	10 wt% PEG 6000 + 17 wt% CA
	Striated fibre surface was obtained	Striated fibre surface was obtained	Striated fibre surface was obtained	Slightly wavy fibre surface was obtained	Striated fibre surface was obtained
2:1 acetone/DMAc	1 wt% AgNO_3 in 17 wt% CA + 10 wt% PEG 200				
	Silver nitrate was reduced to silver nanoparticles and adhered to the fibre surface. The particle size was determined to be ~10 nm.				

Thus, 17 wt% CA in 2:1 acetone/DMAc produced the favourable condition for electrospinning and produced uniform, beadless nanofibers as anticipated. Hence, this solvent system and CA composition was kept fixed in the subsequent stages of the experiment.

Table 7.3 Comparisons of mechanical property

Fibre composition	Stress, MPa
CA	0.002
CA-PEG 200 + 5% citric acid	0.0125
CA-PEG 200 + 10% citric acid	0.033
CA-PEG 200-Ag nanoparticles	0.044

The tensile strength obtained for unmodified CA fibre was significantly lower with a value of 0.002 MPa. However, when modified with 10 wt% citric acid (CT), the stress value increased to 0.033 MPa. With the grafting of Ag nanoparticles in CA fibre, it could sustain higher load and the ultimate tensile strength and elongation at break increased moderately. This is imputed to the fact that Ag nanoparticles acted as stress concentrator in the fibre surface.

Table 7.4 Comparisons of swelling property

Fibre composition	Swelling (%) after 24 hrs
CA	350
CA-PEG 200	650
CA-Ag	400
CA-PEG 200-Ag	600

With the presence of 20% PEG of CA, the ability to retain water increased to 680% which is comparatively higher than the previous value. The water uptake also escalated in presence of PEG with CA/Ag. This phenomenon was attributed to the presence of hydrophilic ethylene glycol unit of PEG performed as hydrogen bond donors/acceptors and could combine with water molecules.

Table 7.5 Comparisons of antibacterial property

Bacterial cell	Mortality (%)	
	CA-PEG 200	CA-PEG 200-Ag
<i>E. coli</i>	0	97.5
<i>S. aureus</i>	-	100

The Ag nanoparticles formed were of 20 nm size which rendered antibacterial properties when tested against *E.coli* and *S.aureus*. Thus, electrospun CA can be a suitable material for wound dressing patches with Ag nanoparticles dispersed along the fibre surface to yield antibacterial activity.

8. CONCLUSION AND RECOMMENDATION

8.1 Findings of the Present Research Work

- a. This work established and analyzed electrospinning of CA with acetic acid, water, acetone, 3:1 acetic acid/water and 2:1 acetone/DMAc as solvent systems which has potential application as a wound dressing material.
- b. 2:1 acetone/DMAc was an apt choice of solvent for CA as it yielded uniform, homogeneous beadless fibres observed from FESEM. The fibre diameter was in the range of 250-400 nm.
- c. However, acetone as a solvent increased the fibre diameter to $\sim 1 \mu\text{m}$ as the fibre morphology appeared to be ribbon-shaped instead of cylindrical. This was due to high volatility of acetone.
- d. Also, electrospinning parameters were investigated also along with solution properties. Voltage of 20 kV and a feed rate of 1.5 ml/h was found to be convenient for this electrospinning process.
- e. After investigating process and solvent properties, a correlation between solubility and spinnability of CA was made using a Teas chart which showed that higher dispersion force (f_d) and lower hydrogen bonding force (f_h) are convenient for both the solubility and spinnability of CA .
- f. Rheological analysis showed that fibre formation improved with increasing viscosity of CA solution.
- g. Electrical conductivity measurement of the CA solutions depicted that with an increase of CA concentration, fibre diameters increased whereas the conductivity decreased.
- h. In the later work, surface modification was achieved using PEG 200. On adding PEG, the surface of the electrospun CA fibres were striated. This was an important modification as the surface roughness will aid in cell attachment of a wound site. Furthermore, PEG also improved swelling behavior necessary for wound exudates absorption. PEG acted as a stabilizing agent of Ag nanoparticles that were formed when AgNO_3 was added into the CA solution and reduced by acetone/DMAc in-situ.
- i. The Ag nanoparticles formed were of 10 nm size which rendered antibacterial properties when tested against gram negative E.coli and gram positive S.aureus.

Thus, electrospun CA can be a suitable material for wound dressing patches with Ag nanoparticles dispersed along the fibre surface to yield antibacterial activity.

8.2 Scope for Future Investigation

The following recommendations for future research work may be suggested:

- a. Different ratios other than 3:1 of acetic acid/water can be tried to observe the electrospinning behaviour and corresponding fibre morphology of CA. Beadless fibres with this solvent system can be an important finding.
- b. In this work, CA fibres have been electrospun in a non-woven mat. As a result, the mechanical properties could not be validated as the fibre alignment were random. Research focus can be made on obtaining fibres with uniaxial direction.
- c. In the present experiment, only PEG 200 has been successfully utilized as a modifying agent. Future research have an opportunity to focus on the higher molecular weight of PEG to bring about changes in the fibre surface properties. However, higher molecular weight PEG renders the polymer solution too viscous to yield. Therefore, electrospinning parameters will have to be varied along with this.
- d. Also, further comprehensive studies can be made on the formation of Ag nanoparticles using different reducing agents and their effect on particle size and the corresponding antibacterial performance.

BIBLIOGRAPHY

- [1] S. Ramakrishna, K. Fujihara, W. Teo, T. Yong, and R. Ramaseshan, "Electrospun nanofibres: solving global issues," vol. 9, no. 3, pp. 40–50, 2006.
- [2] I. S. Chronakis, "Novel nanocomposites and nanoceramics based on polymer nanofibres using electrospinning process - A review," *J. Mater. Process. Technol.*, vol. 167, no. 2–3, pp. 283–293, 2005.
- [3] N. Bhardwaj and S. C. Kundu, "Electrospinning: A fascinating fibre fabrication technique," *Biotechnol. Adv.*, vol. 28, no. 3, pp. 325–347, 2010.
- [4] C. P. Barnes, E. D. Boland, G. E. Wnek, G. L. Bowlin, and K. J. Pawlowski, "Biomedical Nanoscience: Electrospinning Basic Concepts, Applications, and Classroom Demonstration," *MRS Proc.*, vol. 827, pp. 1–12, 2011.
- [5] D. Li and Y. Xia, "Electrospinning of nanofibres: Reinventing the wheel?," *Adv. Mater.*, vol. 16, no. 14, pp. 1151–1170, 2004.
- [6] Z. M. Huang, Y. Z. Zhang, M. Kotaki, and S. Ramakrishna, "A review on polymer nanofibres by electrospinning and their applications in nanocomposites," *Compos. Sci. Technol.*, vol. 63, no. 15, pp. 2223–2253, 2003.
- [7] S. A. Theron, E. Zussman, and A. L. Yarin, "Experimental investigation of the governing parameters in the electrospinning of polymer solutions," *Polymer (Guildf.)*, vol. 45, no. 6, pp. 2017–2030, 2004.
- [8] C. Mit-Uppatham, M. Nithitanakul, and P. Supaphol, "Ultrafine electrospun polyamide-6 fibres: Effect of solution conditions on morphology and average fibre diameter," *Macromol. Chem. Phys.*, vol. 205, no. 17, pp. 2327–2338, 2004.
- [9] P. Supaphol, C. Mit-uppatham, and M. Nithitanakul, "Ultrafine electrospun polyamide-6 fibres: Effects of solvent system and emitting electrode polarity on morphology and average fibre diameter," *Macromol. Mater. Eng.*, vol. 290, no. 9, pp. 933–942, 2005.
- [10] S. L. Shenoy, W. D. Bates, and G. Wnek, "Correlations between electrospinnability and physical gelation," *Polymer (Guildf.)*, vol. 46, no. 21, pp. 8990–9004, 2005.
- [11] H. Fong, I. Chun and D. H. Renekar, "Beaded nanofibers formed during electrospinning," *Polymer*, vol. 40, no. 16, pp.4585-4592, 1999.
- [12] J. H. He, Y. Q. Wan, and J. Y. Yu, "Application of vibration technology to polymer electrospinning," *Int. J. Nonlinear Sci. Numer. Simul.*, vol. 5, no. 3, pp. 253–262, 2004.
- [13] I. Sas, R. E. Gorga, J. A. Joines, and K. A. Thoney, "Literature review on superhydrophobic self-cleaning surfaces produced by electrospinning," *J. Polym. Sci. Part B Polym. Phys.*, vol. 50, no. 12, pp. 824–845, 2012.
- [14] B. Condon, A. P. S. Sawhney, D. Hui, K. V. Singh, S. S. Pang, and G. Li, "Modern Applications of Nanotechnology in Textiles," *Text. Res. J.*, vol. 78, no.

- 8, pp. 731–739, 2008.
- [15] G. C. Rutledge and S. V. Fridrikh, “Formation of fibres by electrospinning,” *Adv. Drug Deliv. Rev.*, vol. 59, no. 14, pp. 1384–1391, 2007.
- [16] S. Agarwal, J. H. Wendorff, and A. Greiner, “Use of electrospinning technique for biomedical applications,” *Polymer (Guildf.)*, vol. 49, no. 26, pp. 5603–5621, 2008.
- [17] E. R. Kenawy, G. L. Bowlin, K. Mansfield, J. Layman, D. G. Simpson, E. H. Sanders and G. E. Wnek “Release of tetracycline hydrochloride from electrospun poly(ethylene-co-vinylacetate), poly(lactic acid), and a blend,” *J. Control. Release*, vol. 81, no. 1–2, pp. 57–64, 2002.
- [18] M. Gouda, A. Aljaafari, and M. A. Al-Omair, “Functional electrospun cellulosic nanofibre mats for antibacterial bandages,” *Fibres Polym.*, vol. 18, no. 12, pp. 2379–2386, 2017.
- [19] I. D. Norris, M. M. Shaker, F. K. Ko, and A. G. MacDiarmid, “Electrostatic fabrication of ultrafine conducting fibres: Polyaniline/polyethylene oxide blends,” *Synth. Met.*, vol. 114, no. 2, pp. 109–114, 2000.
- [20] C. Shao, H. Y. Kim, J. Gong, B. Ding, D. R. Lee, and S. J. Park, “Fibre mats of poly(vinyl alcohol)/silica composite via electrospinning,” *Mater. Lett.*, vol. 57, no. 9–10, pp. 1579–1584, 2003.
- [21] M. M. Hohman, M. Shin, G. Rutledge, and M. P. Brenner, “Electrospinning and electrically forced jets. II. Applications,” *Phys. Fluids*, vol. 13, no. 8, pp. 2221–2236, 2001.
- [22] K. Graham, M. Ouyang, T. Raether, T. Grafe, B. McDonald, and P. Knauf, “Polymeric nanofibers in air filtration application,” In *Fifteenth Annual Technical Conference & Expo of the American Filtration & Separations Society, Galveston, Texas*, pp. 9-12, 2002.
- [23] P. P. Tsai, H. Schreuder-Gibson and P. Gibson, “Different electrostatic methods for making electret filters,” *Journal of Electrostatics*, vol. 54, no. 3-4, pp. 333-341, 2002.
- [24] R. Mathers, D. A. Czaplowski, H. G. Craighead, J. Kameoka, and G. W. Coates, “Nanofluidic channels with elliptical cross sections formed using a nonlithographic process,” *Appl. Phys. Lett.*, vol. 83, no. 23, pp. 4836–4838, 2003.
- [25] H. Hou, Z. Jun, A. Reuning, A. Schaper, J. H. Wendorff, and A. Greiner, “Poly(p-xylylene) nanotubes by coating and removal of ultrathin polymer template fibres,” *Macromolecules*, vol. 35, no. 7, pp. 2429–2431, 2002.
- [26] M. Bognitzki et al., “Preparation of fibres with nanoscaled morphologies: Electrospinning of polymer blends,” *Polym. Eng. Sci.*, vol. 41, no. 6, pp. 982–989, 2004.
- [27] K. Ohgo, C. Zhao, M. Kobayashi, and T. Asakura, “Preparation of non-woven nanofibres of Bombyx mori silk, Samia cynthia ricini silk and recombinant hybrid silk with electrospinning method,” *Polymer (Guildf.)*, vol. 44, no. 3, pp. 841–846, 2002.

- [28] G. E. Wnek, M. E. Carr, D. G. Simpson, and G. L. Bowlin, "Electrospinning of nanofibre fibrinogen structures," *Nano Lett.*, vol. 3, no. 2, pp. 213–216, 2003.
- [29] W.G. Glasser, "Prospects for future applications of cellulose acetate," *Macromolecular Symposia*, vol. 208 (1), pp. 371-394, 2004.
- [30] D. Haas, S. Heinrich, and P. Greil, "Solvent control of cellulose acetate nanofibre felt structure produced by electrospinning," pp. 1299–1306, 2010.
- [31] S. Tungprapa et al., "Electrospun cellulose acetate fibres: Effect of solvent system on morphology and fibre diameter," *Cellulose*, vol. 14, no. 6, pp. 563–575, 2007.
- [32] Z. Ma and S. Ramakrishna, "Electrospun regenerated cellulose nanofibre affinity membrane functionalized with protein A / G for IgG purification," vol. 319, pp. 23–28, 2008.
- [33] S. De Vrieze, T. Van Camp, A. Nelvig, B. Hagström, P. Westbroek and Karen De Clerck, "The effect of temperature and humidity on electrospinning," *J. Mat. Sci.*, vol. 44, no. 5, pp. 1357–1362, 2009.
- [34] S. Zalipsky, L. Technology, H. Court, M. Park, and C. R. August, "Functionalized Poly(ethylene glycol) for Preparation of Biologically Relevant Conjugates," *Bioconjugate Chem.*, vol. 6, no. 2, pp. 150–165, 1995.
- [35] P. Gibson and H. Schreuder-gibson, "Patterned Electrospun Polymer Fibre Structures," *e-Polym.*, vol. 2, pp. 1-15, 2003
- [36] J. A. Matthews, E. D. Boland, G. E. Wnek, D. G. Simpson, and G. L. Bowlin, "Electrospinning of collagen type II: a feasibility study," *Journal of bioactive and compatible polymers*, vol. 18, no. 2, pp. 125-134, 2003.
- [37] D. E. Bruns, "Oxidation of polyethylene glycols by alcohol dehydrogenase." *Biochemical pharmacology*, vol. 38, no. 1, pp. 73-76, 1989.
- [38] D. Shi, "Effect of polyethylene glycol on the antibacterial properties of polyurethane/carbon nanotube electrospun nanofibers. *RSC advances*, vol. 6, no. 23, pp. 19238-19244, 2016.
- [39] D. V Goia and D. V Goia, "Preparation and formation mechanisms of uniform metallic particles in homogeneous solutions," *J. mater. Chem.*, vol. 14, no. 4, pp.

451–458, 2004.

- [40] K. M. M. A. El-nour, A. Al-warthan, and R. A. A. Ammar, “Synthesis and applications of silver nanoparticles,” *Arab. J. Chem.*, vol. 3, no. 3, pp. 135–140, 2010.
- [41] Z. Chen and L. Gao, “A facile and novel way for the synthesis of nearly monodisperse silver nanoparticles,” *Mater. Res. Bull.*, vol. 42, pp. 1657–1661, 2007.
- [42] M. Popa, T. Pradell, D. Crespo, and M. Calder, “Stable silver colloidal dispersions using short chain polyethylene glycol,” *Colloids and Surfaces A: Physicochemical and Engineering Aspects*, vol. 303, pp. 184–190, 2007.
- [43] C. Luo, Y. Zhang, X. Zeng, Y. Zeng, and Y. Wang, “The role of poly (ethylene glycol) in the formation of silver nanoparticles,” vol. 288, pp. 444–448, 2005.
- [44] A. Shkilnyy and M. Souc, “Poly (ethylene glycol) -stabilized silver nanoparticles for bioanalytical applications of SERS spectroscopy,” *Journal of colloid and interface science*, vol. 288, no. 2, pp. 1868–1872, 2009.
- [45] B. Sciences and J. A. Building, “Wound Healing Dressings and Drug Delivery Systems : A Review,” *Journal of pharmaceutical sciences*, vol. 97, no. 8, pp. 2892–2923, 2008.
- [46] A. E. Rivera and J. M. Spencer, “Clinical aspects of full-thickness wound healing,” *Clinics in dermatology*, vol. 25, no. 1, pp. 39–48, 2007.
- [47] M. K. Strecker-mcgraw, T. R. Jones, D. G. Baer, T. R. Jones, and D. G. Baer, “Soft Tissue Wounds and Principles of Healing,” *Emergency medicine clinics of North America*, vol. 25, pp. 1–22, 2007.
- [48] Y. Zhang, C. T. Lim, and S. Ramakrishna, “Recent development of polymer nanofibres for biomedical and biotechnological applications,” *Journal of Materials Science: Materials in Medicine*, vol. 6, pp. 933–946, 2005.
- [49] N. Sirelkhatim, D. LaJeunesse, A. D. Kelkar and L. Zhang, "Antifungal activity of amidoxime surface functionalized electrospun polyacrylonitrile nanofibers," *Mater. Lett.*, vol. 141, pp.217-220, 2015

- [50] A. Akhgari, Z. Shakib and S. Sanati, " A review on electrospun nanofibers for oral drug delivery," *Nanomedicine Journal*, vol. 4, no. 4, pp. 197-207, 2017.
- [51] M. Raffi, F. Hussain, T. M. Bhatti, J. Akhter, A. Hameed and M. M. Hasan, "Antibacterial Characterization of Silver Nanoparticles against *E. coli* ATCC-15224," *Journal of materials science and technology*, vol. 24, no. 2, pp. 192–196, 2008.
- [52] A. B. Smetana, K. J. Klabunde, and C. M. Sorensen, "Synthesis of spherical silver nanoparticles by digestive ripening , stabilization with various agents , and their 3-D and 2-D superlattice formation," *Journal of colloid and interface science*, vol. 284, pp. 521–526, 2005.
- [53] L. Kvitek, J. Soukupova, R. Vec, R. Prucek, M. Holecova, and R. Zbor, "Effect of Surfactants and Polymers on Stability and Antibacterial Activity of Silver Nanoparticles (NPs)," *The Journal of Physical Chemistry C*, vol. 112, no. 15, pp. 5825–5834, 2008.
- [54] G. K. Vertelov, Y. A. Krutyakov, O. V Efremenkova, and A. Y. Olenin, "A versatile synthesis of highly bactericidal Myramistin[®] stabilized silver nanoparticles," *Nanotechnology*, vol. 19, no. 25, pp. 355707, 2008.
- [55] K. I. Y. Yoon, J. H. Byeon, C. W. O. O. Park, and J. Hwang, "Antimicrobial Effect of Silver Particles on Bacterial Contamination of Activated Carbon Fibres," *Environmental science & technology*, vol. 42, no. 4, pp. 1251–1255, 2008.
- [56] Y. Zhang, H. Peng, W. Huang, Y. Zhou, and D. Yan, "Facile preparation and characterization of highly antimicrobial colloid Ag or Au nanoparticles," *Journal of Colloid and Interface Science*, vol. 325, pp. 371–376, 2008.
- [57] S. Choi, Y. Zhang, A. Gopalan, K. Lee, and H. Kang, "Preparation of catalytically efficient precious metallic colloids by γ -irradiation and characterization," *Colloids and Surfaces A: Physicochemical and Engineering Aspects*, vol. 256, pp. 165–170, 2005.
- [58] Z. Li, Y. Li, X. Qian, J. Yin, and Z. Zhu, "A simple method for selective immobilization of silver nanoparticles," *Applied Surface Science*, vol. 250, pp. 109–116, 2005.

- [59] A. S. Gurav, T. T. K. T, L. Wang, E. I. Kauppinen, and J. Joutsensaari, "Generation of nanometer-size fullerene particles via vapor condensation," *Chemical Phy. Lett.*, vol. 218, no. 4, pp. 304–308, 1994.
- [60] F. Einar, H. Fissan, and B. Rellinghaus, "Sintering and evaporation characteristics of gas-phase synthesis of size-selected PbS nanoparticles," *Mater. Sci. Engg. B*, vol. 70, pp. 329–334, 2000.
- [61] J. Hee, H. Cheol, H. Soo, J. Ho, and S. Soo, "Metal nanoparticle generation using a small ceramic heater with a local heating area," *Journal of Aerosol Science*, vol. 37, pp. 1662–1670, 2006.
- [62] F. Mafune, J. Kohno, Y. Takeda, and T. Kondow, "Formation and Size Control of Silver Nanoparticles by Laser Ablation in Aqueous Solution," *The Journal of Physical Chemistry B*, vol. 104, no.39, pp. 9111–9117, 2000.
- [63] M. Meunier, "Synthesis of colloidal nanoparticles during femtosecond laser ablation of gold in water Synthesis of colloidal nanoparticles during femtosecond laser ablation of gold in water," *Journal of Applied Physics*, vol. 94, no. 12, pp. 10–13, 2014.
- [64] C. Hwang, Y. S. Fu, Y. L. Lu, S. W. Jang, P. T. Chou, C. C. Wang and S. J. Yu "Synthesis , Characterization , and Highly Efficient Catalytic Reactivity of Suspended Palladium Nanoparticles," *Journal of Catalysis*, .vol. 341, pp. 336–341, 2000.
- [65] S. Kim, B. K. Yu, K. Chun and W. Kang "Catalytic effect of laser ablated Ni nanoparticles in the oxidative addition reaction for a coupling reagent of benzylchloride and bromoacetonitrile," *Journal of Molecular Catalysis A: Chemical*, vol. 226, pp. 231–234, 2005.
- [66] A. V Simakin, V. V Voronov, G. A. Shafeev, and R. Brayner, "Nanodisks of Au and Ag produced by laser ablation in liquid environment," *Chemical Physics Letters*, vol. 348, no. November, pp. 182–186, 2001.
- [67] T. Tsuji, K. Iryo, N. Watanabe, and M. Tsuji, "Preparation of silver nanoparticles by laser ablation in solution : influence of laser wavelength on particle size," *Applied Surface Science*, vol. 202, pp. 80–85, 2002.

- [68] A. Tao, P. Sinsermsuksakul and P. Yang “Polyhedral Silver Nanocrystals with Distinct Scattering Signatures,” *Angewandte Chemie International Edition*, vol. 45, no. 28 , pp. 4597–4601, 2006.
- [69] U. Nickel, A. Castell, K. Po, and S. Schneider, “A Silver Colloid Produced by Reduction with Hydrazine as Support for Highly Sensitive Surface-Enhanced Raman,” *Langmuir*, vol. 23, no. 14, pp. 9087–9091, 2000.
- [70] C. Lee and D. Meisel, “Adsorption and Surface-Enhanced Raman of Dyes on Silver and Gold Sols’,” *The Journal of Physical Chemistry*, vol. 86, no. 17, pp. 3391–3395, 1982.
- [71] J. Bai, Y. Li, J. Du, S. Wang, J. Zheng and Q, Yang “One-pot synthesis of polyacrylamide-gold nanocomposite,” *Materials Chemistry and Physics*, vol. 106, pp. 412–415, 2007.
- [72] M. M. Oliveira, D. Ugarte, D. Zanchet, and A. J. G. Zarbin, “Influence of synthetic parameters on the size , structure , and stability of dodecanethiol-stabilized silver nanoparticles,” *Journal of Colloid and Interface Science*, vol. 292, pp. 429–435, 2005.
- [73] Z. S. Pillai and P. V Kamat, “What Factors Control the Size and Shape of Silver Nanoparticles in the Citrate Ion Reduction Method,” *The Journal of Physical Chemistry B*, vol. 108, no. 3, pp. 945–951, 2004.
- [74] P. A. Buffat, “Electron diffraction and HRTEM studies of multiply-twinned structures and dynamical events in metal nanoparticles : facts and artefacts,” *Materials Chemistry and Physics*, vol. 81, pp. 368–375, 2003.
- [75] S. May and A. Ben-shaul, “Molecular Theory of the Sphere-to-Rod Transition and the Second CMC in Aqueous Micellar Solutions,” *The Journal of Physical Chemistry B*, vol. 105, no. 3, pp. 630–640, 2001.
- [76] H. Huang and Y. Yang, “Science and Preparation of silver nanoparticles in inorganic clay suspensions,” *Compos. Sci. Technol.*, vol. 68, no. 14, pp. 2948–2953, 2008.
- [77] L. Yu, “Environment friendly fluid loss additives to protect the marine environment from the detrimental effect of mud additives,” *Journal of Petroleum*

- Science and Engineering, vol. 48, pp. 199–208, 2005.
- [78] P. Raveendran, J. Fu, S. L. Wallen, C. Hill, and N. Carolina, “Completely “Green” Synthesis and Stabilization of Metal Nanoparticles,” *Journal of the American Chemical Society*, vol. 125, no. 46, pp. 13940–13941, 2003.
- [79] A. R. Vilchis-nestor, V. Sánchez-mendieta, M. A. Camacho-lópez, R. M. Gómez-espinosa, M. A. Camacho-lópez, and J. A. Arenas-alatorre, “Solventless synthesis and optical properties of Au and Ag nanoparticles using *Camellia sinensis* extract,” *Mat. Lett.* vol. 62, pp. 3103–3105, 2008.
- [80] N. Li, “Toxic Potential of Materials at the Nanolevel,” *Science*, vol. 311, no.5761, pp. 622–628, 2006.
- [81] E. Mendis, N. Rajapakse, H. Byun, and S. Kim, “Investigation of jumbo squid (*Dosidicus gigas*) skin gelatin peptides for their in vitro antioxidant effects,” *Life Sciences*, vol. 77, pp. 2166–2178, 2005.
- [82] S. J. Stohs and D. Bagchil, “Oxidative mechanisms in the toxicity of metal ions,” *Free Radical Biology and Medicine*, vol. 18, no. 2, pp. 321–336, 1995.
- [83] C. Carlson, S. M. Hussain, A. M. Schrand, K. L. Hess, R. L. Jones, and J. J. Schlager, “Unique Cellular Interaction of Silver Nanoparticles : Size-Dependent Generation of Reactive Oxygen Species,” *The Journal of Physical Chemistry B* , vol 112, no. 43, pp. 13608–13619, 2008.
- [84] H. Park, “Silver-ion-mediated reactive oxygen species generation affecting bactericidal activity,” *Water Res.*, vol. 43, no. 4, pp. 1027–1032, 2009.
- [85] J. R. Morones, J. L. Elechiguerra, A. Camacho, and K. Holt, “The bactericidal effect of silver nanoparticles,” *Nanotechnology*, vol. 16, no. 10, pp. 2346, 2005.
- [86] X. N. Xu, W. J. Brownlow, S. V Kyriacou, Q. Wan, and J. J. Viola, “Real-Time Probing of Membrane Transport in Living Microbial Cells Using Single Nanoparticle Optics and Living Cell Imaging,” *Biochemistry*, vol. 43, no. 32, pp. 10400–10413, 2004.
- [87] R. Konwarh, N. Karak, and M. Misra, “Electrospun cellulose acetate nanofibres: The present status and gamut of biotechnological applications,” *Biotechnol. Adv.*, vol. 31, no. 4, pp. 421–437, 2013.

- [88] M. Wu, R. Liu, Y. Li and R. Wu, "Electrospun membrane of cellulose acetate for heavy metal ion adsorption in water treatment," *Carbohydr. Polym.*, vol. 83, pp. 743-748, 2011.
- [89] Z. Ma, M. Kotaki and S. Ramakrishna, "Electrospun cellulose nanofiber as affinity membrane," *Journal of Membrane Science*, vol. 265, pp. 115-123, 2005.
- [90] S. H. Tan, R. Inai, M. Kotaki and S. Ramakrishna, "Systematic parameter study for ultra-fine fiber fabrication via electrospinning process," *Polym.*, vol. 46, pp. 6128-6134, 2005.
- [91] K. Khoshnevisan et al., "Cellulose acetate electrospun nanofibres for drug delivery systems: Applications and recent advances," *Carbohydr. Polym.*, vol. 198, pp. 131–141, 2018.
- [92] B. Tarus, N. Fadel, A. Al-oufy, and M. El-messiry, "Effect of polymer concentration on the morphology and mechanical characteristics of electrospun cellulose acetate and poly (vinyl chloride) nanofibre mats," *Alexandria Eng. J.*, 2016.
- [93] S. Agarwal, J. H. Wendorff, and A. Greiner, "Use of electrospinning technique for biomedical applications," *Polymer (Guildf.)*, vol. 49, no. 26, pp. 5603–5621, 2008.
- [94] S. L. Shenoy, W. D. Bates, and G. Wnek, "Correlations between electrospinnability and physical gelation," *Polymer (Guildf.)*, vol. 46, no. 21, pp. 8990–9004, 2005.
- [95] T. D. Brown, P. D. Dalton, and D. W. Hutmacher, "Melt electrospinning today: An opportune time for an emerging polymer process," *Prog. Polym. Sci.*, vol. 56, pp. 116–166, 2016.
- [96] T. Lan, "Electrospun nanofibrous cellulose diacetate nitrate membrane for protein separation," *J. Memb. Sci.*, vol. 489, pp. 204–211, 2015.
- [97] S. Li, N. Jia, M. Ma, Z. Zhang, Q. Liu, and R. Sun, "Cellulose – silver nanocomposites : Microwave-assisted synthesis , characterization , their thermal stability , and antimicrobial property," *Carbohydr. Polym.*, vol. 86, no. 2, pp. 441–447, 2011.

- [98] H. Liu and C. Tang, "Electrospinning of Cellulose Acetate in Solvent Mixture N,N-Dimethylacetamide (DMAc)/Acetone," *Polym. J.*, vol. 39, no. 1, pp. 65–72, 2007.
- [99] A. Celebioglu and T. Uyar, "Electrospun porous cellulose acetate fibres from volatile solvent mixture," *Mater. Lett.*, vol. 65, no. 14, pp. 2291–2294, 2011.
- [100] Y. Marcus, "Total and partial solubility parameters of sub- and supercritical ethanol," *J. Chem. Thermodyn.*, vol. 126, no. June, pp. 187–189, 2018.
- [101] F. Klar and N. A. Urbanetz, "Solubility parameters of hypromellose acetate succinate and plasticization in dry coating procedures," *Drug Dev. Ind. Pharm.*, vol. 42, no. 10, pp. 1621–1635, 2016.
- [102] C. J. Luo, M. Nangrejo, and M. Edirisinghe, "A novel method of selecting solvents for polymer electrospinning," *Polymer (Guildf.)*, vol. 51, no. 7, pp. 1654–1662, 2010.
- [103] M. M. Mahmud, A. Perveen, M. A. Matin and M. T. Arafat, " Effects of binary solvent mixture on the electrospinning behavior of poly(vinyl alcohol)," *Mater. Res. Exp.*, vol. 5, no.11, pp. 1-23, 2018
- [104] J. Lasprilla-Botero, M. Álvarez-Láinez, and J. M. Lagaron, "The influence of electrospinning parameters and solvent selection on the morphology and diameter of polyimide nanofibres," *Mater. Today Commun.*, vol. 14, no. November 2017, pp. 1–9, 2018.
- [105] S. Huan, "Effect of experimental parameters on morphological, mechanical and hydrophobic properties of electrospun polystyrene fibres," *Materials (Basel)*, vol. 8, no. 5, pp. 2718–2734, 2015.
- [106] B. Ghorani, S. J. Russell, and P. Goswami, "Controlled morphology and mechanical characterisation of electrospun cellulose acetate fibre webs," *Int. J. Polym. Sci.*, vol. 2013, pp. 1-12, 2013.
- [107] M. M. Batista, R. Guirardello, and M. A. Krähenbühl, "Determination of the Hansen Solubility Parameters of Vegetable Oils, Biodiesel, Diesel, and Biodiesel–Diesel Blends," *J. Am. Oil Chem. Soc.*, vol. 92, no. 1, pp. 95–109,

2015.

- [108] T. L. Lee and C. T. Lo, “Photoresponsive and fluorescence behaviors of azobenzene-containing amphiphilic block copolymers,” *J. Polym. Sci. Part B Polym. Phys.*, vol. 55, no. 10, pp. 793–803, 2017.
- [109] C. Angammana, *A Study of the Effects of Solution and Process Parameters on the Electrospinning Process and Nanofibre Morphology*, PhD Thesis, vol. 47, no. 3, pp. 1109–1117, 2011.
- [110] M. M. Hohman, M. Shin, G. Rutledge, and M. P. Brenner, “Electrospinning and electrically forced jets. II. Applications,” *Phys. Fluids*, vol. 13, no. 8, pp. 2221–2236, 2001.
- [111] I. W. Fathona and A. Yabuki, “Mapping the influence of electrospinning parameters on the morphology transition of short and continuous nanofibres,” *Fibres Polym.*, vol. 17, no. 8, pp. 1238–1244, 2016.
- [112] Y. K. Wu, L. Wang, J. Fan, W. Shou, B. M. Zhou, and Y. Liu, “Multi-jet electrospinning with auxiliary electrode: The influence of solution properties,” *Polymers (Basel)*, vol. 10, no. 6, 2018.
- [113] N. Hoogesteijn Von Reitzenstein, X. Bi, Y. Yang, K. Hristovski, and P. Westerhoff, “Morphology, structure, and properties of metal oxide/polymer nanocomposite electrospun mats,” *J. Appl. Polym. Sci.*, vol. 133, no. 33, pp. 1–9, 2016.
- [114] S. Wu, X. Qin, and M. Li, “The structure and properties of cellulose acetate materials: A comparative study on electrospun membranes and casted films,” *J. Ind. Text.*, vol. 44, no. 1, pp. 85–98, 2014.
- [115] J. Stanger, N. Tucker, K. Kirwan, and M. P. Staiger, “Effect of Charge Density on the Taylor Cone in Electrospinning,” *Int. J. Mod. Phys. B*, vol. 23, no. 6, pp. 1956–1961, 2009.
- [116] D. Liang, B. S. Hsiao, and B. Chu, “Functional electrospun nanofibrous scaffolds for biomedical applications,” *Adv. Drug Deliv. Rev.*, vol. 59, no. 14, pp. 1392–1412, 2007.
- [117] M. Zhang, X. H. Li, Y. D. Gong, N. M. Zhao, and X. F. Zhang, “Properties and

- biocompatibility of chitosan films modified by blending with PEG,” *Biomaterials*, vol. 23, no. 13, pp. 2641–2648, 2002.
- [118] S. Majumder, A. Matin, A. Sharif and M. T. Arafat, “Understanding solubility, spinnability and electrospinning behaviour of cellulose acetate using different solvent systems,” *Bull. Mater. Sci.* In press 2019.
- [119] C. Chen, L. Wang, and Y. Huang, “Electrospun phase change fibres based on polyethylene glycol / cellulose acetate blends,” *Appl. Energy*, vol. 88, no. 9, pp. 3133–3139, 2011.
- [120] S. Li, N. Jia, M. Ma, Z. Zhang, Q. Liu, and R. Sun, “Cellulose – silver nanocomposites : Microwave-assisted synthesis , characterization , their thermal stability , and antimicrobial property,” *Carbohydr. Polym.*, vol. 86, no. 2, pp. 441–447, 2011.
- [121] B. Wang, J. Chen, H. Peng, J. Gai, J. Kang, and Y. Cao, “Investigation on Changes in the Miscibility, Morphology, Rheology and Mechanical Behavior of Melt Processed Cellulose Acetate through Adding Polyethylene Glycol as a Plasticizer,” *J. Macromol. Sci. Part B Phys.*, vol. 55, no. 9, pp. 894–907, 2016.
- [122] M. W. Frey, “Electrospinning cellulose and cellulose derivatives,” *Polym. Rev.*, vol. 48, no. 2, pp. 378–391, 2008.[36]
- [123] W. L. Chou, D. G. Yu, M. C. Yang, and C. H. Jou, “Effect of molecular weight and concentration of PEG additives on morphology and permeation performance of cellulose acetate hollow fibres,” *Sep. Purif. Technol.*, vol. 57, no. 2, pp. 209–219, 2007.
- [124] C. Chen, L. Wang, and Y. Huang, “Electrospun phase change fibres based on polyethylene glycol / cellulose acetate blends,” *Appl. Energy*, vol. 88, no. 9, pp. 3133–3139, 2011.
- [125] C. Chen, L. Wang, and Y. Huang, “Electrospun phase change fibres based on polyethylene glycol / cellulose acetate blends,” *Appl. Energy*, vol. 88, no. 9, pp. 3133–3139, 2011.
- [126] W. Cui, X. Li, S. Zhou, and J. Weng, “Degradation patterns and surface wettability of electrospun fibrous mats.” *Polymer Degradation and Stability*, vol.

93, no. 3, pp.731-738, 2008

- [127] R. R. M. de Freitas, A. M. Senna, and V. R. Botaro, "Influence of degree of substitution on thermal dynamic mechanical and physicochemical properties of cellulose acetate," *Ind. Crops Prod.*, vol. 109, no. August, pp. 452–458, 2017.
- [128] H. Yu, "Novel porous three-dimensional nanofibrous scaffolds for accelerating wound healing," *Chem. Eng. J.*, 2019.
- [129] R. Ramalingam, "Poly- ϵ -Caprolactone/Gelatin Hybrid Electrospun Composite Nanofibrous Mats Containing Ultrasound Assisted Herbal Extract: Antimicrobial and Cell Proliferation Study," *Nanomaterials*, vol. 9, no. 3, p. 462, 2019.
- [130] K. A. Rieger, N. P. Birch, and J. D. Schiffman, "Designing electrospun nanofibre mats to promote wound healing-a review," *J. Mater. Chem. B*, vol. 1, no. 36, pp. 4531–4541, 2013.
- [131] M. Mazur, "Electrochemically prepared silver nanoflakes and nanowires," *Electrochem. commun.*, vol. 6, no. 4, pp. 400–403, 2004.
- [132] Z. Jian, Z. Xiang, and W. Yongchang, "Electrochemical synthesis and fluorescence spectrum properties of silver nanospheres," *Microelectron. Eng.*, vol. 77, no. 1, pp. 58–62, 2005.
- [133] V. Vignesh, K. Felix Anbarasi, S. Karthikeyeni, G. Sathiyarayanan, P. Subramanian, and R. Thirumurugan, "A superficial phyto-assisted synthesis of silver nanoparticles and their assessment on hematological and biochemical parameters in *Labeo rohita* (Hamilton, 1822)," *Colloids Surfaces A Physicochem. Eng. Asp.*, vol. 439, pp. 184–192, 2013.
- [134] Y. Li and F. Chu, "Research on the preparation of silver nanoparticles by chemical reduction method," *Lect. Notes Electr. Eng.*, vol. 417, pp. 1109–1114, 2017.
- [135] S. Kendouli, "Modification of cellulose acetate nanofibres with PVP/Ag addition," *Mater. Sci. Semicond. Process.*, vol. 28, pp. 13–19, 2014.
- [136] M. Gopiraman, "Silver coated anionic cellulose nanofibre composites for an efficient antimicrobial activity," *Carbohydr. Polym.*, vol. 149, pp. 51–59, 2016.

- [137] K. Kalwar, L. Hu, D. L. Li, and D. Shan, "AgNPs incorporated on deacetylated electrospun cellulose nanofibres and their effect on the antimicrobial activity," *Polym. Adv. Technol.*, vol. 29, no. 1, pp. 394–400, 2018.
- [138] W. K. Son, J. H. Youk, and W. H. Park, "Antimicrobial cellulose acetate nanofibres containing silver nanoparticles," *Carbohydr. Polym.*, vol. 65, no. 4, pp. 430–434, 2006.
- [139] K. Hyuk Jang, Y. Joon Yu, Y. Ha Lee, Y. Ok Kang, and W. Ho Park, "Antimicrobial activity of cellulose-based nanofibres with different Ag phases," *Mater. Lett.*, vol. 116, pp. 146–149, 2013.
- [140] K. R. Aadil, S. I. Mussatto, and H. Jha, "Synthesis and characterization of silver nanoparticles loaded poly (vinyl alcohol)-lignin electrospun nanofibers and their antimicrobial activity," *Int. J. Biol. Macromol.*, vol. 120, pp. 763-767, 2018.

